Epigenetic regulation of normal human mammary cell type specific miRNAs

Lukas Vrba[1,4], James C. Garbe[3], Martha R. Stampfer[1,3], Bernard W. Futscher[1,2,*]

[1]Arizona Cancer Center, The University of Arizona, Tucson, AZ 85724, USA

[2]Department of Pharmacology & Toxicology, College of Pharmacy, The University of Arizona, Tucson, AZ 85724, USA

[3]Life Sciences Division; Lawrence Berkeley National Laboratory, Berkeley, CA 94720 USA

[4]Biology Centre ASCR, v.v.i., Institute of Plant Molecular Biology, Ceske Budejovice, 37005, Czech Republic

*Corresponding Author:

Bernard W. Futscher

Arizona Cancer Center

1515 N Campbell Ave

Tucson, AZ 85724

Email: (bfutscher@azcc.arizona.edu)

Phone: 520-626-4646

Fax: 520-626-4979

Running Title: Epigenetic regulation of miRNAs

Keywords:

miRNA, epigenetic, DNA methylation, histone, H3K27me3, H3K4me3, acetylation, promoter

DISCLAIMER

ABSTRACT

Epigenetic mechanisms are important regulators of cell type specific genes, including miRNAs. In order to identify cell type specific miRNAs regulated by epigenetic mechanisms, we undertook a global analysis of miRNA expression and epigenetic states in three isogenic pairs of human mammary epithelial cells (HMEC) and human mammary fibroblasts (HMF), which represent two differentiated cell types typically present within a given organ, each with a distinct phenotype and a distinct epigenotype. While miRNA expression and epigenetic states showed strong interindividual concordance within a given cell type, almost 10% of the expressed miRNA showed a cell type specific pattern of expression that was linked to the epigenetic state of their promoter. The tissue specific miRNA genes were epigenetically repressed in non-expressing cells by DNA methylation (38%) and H3K27me3 (58%) with only a small set of miRNAs (21%) showing a dual epigenetic repression where both DNA methylation and H3K27me3 were present at their promoters, such as *MIR10A* and *MIR10B*. Individual miRNA clusters of closely related miRNA gene families can each display cell type specific repression by the same or complementary epigenetic mechanisms, such as the *MIR200* family and *MIR205*, where fibroblasts repress *MIR200C/141* by DNA methylation, *MIR200A/200B/429* by H3K27me3, and *MIR205* by both DNA methylation and H3K27me3. Since deregulation of many of the epigenetically regulated miRNAs we identified have been linked to disease processes, such as cancer, it is predicted that compromise of the epigenetic control mechanisms is important for this process. Overall, these results highlight the importance of epigenetic regulation in the control of normal cell type specific miRNA expression.

[Supplemental material is available for this article.]

INTRODUCTION

MicroRNAs (miRNA) are short single-stranded RNA molecules that regulate gene expression at the posttranscriptional level by inhibiting translation of target mRNAs or by stimulating their degradation. Mature miRNAs are processed from hairpin precursors that are either encoded by dedicated miRNA genes that are often found in clusters, or they reside in the introns of protein coding genes and are processed following transcription of the host gene. According to current estimates there are over a thousand miRNAs expressed from over five hundred transcriptional units (miRNA genes) encoded in the human genome. These miRNAs control, in part, the expression of about two thirds of human genes (Friedman et al. 2009). miRNAs are involved in determination of cell identity and their expression is often deregulated in cancer (Peter 2009), however, relatively little is known about how their expression is regulated. Evidence is emerging that similar to protein-coding genes, epigenetic mechanisms play an important role in this process (Iorio et al. 2010).

Epigenetic mechanisms involve DNA methylation and posttranslational modifications of chromatin proteins, including histones. 5-methylcytosine residues are a feature of transcriptionally silent heterochromatin and this epigenetic mark is indispensable for mammalian development; it participates in X chromosome inactivation, gene imprinting, and control of cell type specific gene expression patterns (Bird 2002; Lister et al. 2009; Laurent et al. 2010). Methyl groups are deposited on CpG cytosine residues by de novo DNA methyltransferases,

DNMT3A and DNMT3B, and then maintained by DNA methyltransferase DNMT1 (Jaenisch and Bird 2003; Miranda and Jones 2007). In addition to DNA methylation there exist a number of posttranslational modifications on histones that act as positive or negative epigenetic regulators of gene expression. Two major repressive histone marks commonly present in euchromatin regions are trimethylation of histone H3 at lysine 27 (H3K27me3) and dimethylation of histone H3 at lysine 9 (H3K9me2). The H3K27me3 modification is deployed by the histone methyltransferase EZH2, a part of the polycomb repressive complex 2 (PRC2) (Simon and Kingston 2009). The H3K9me2 repressive histone modification is deposited by G9a, a member of the H3K9 specific histone methyltransferases (Tachibana et al. 2002). Two major permissive marks are trimethylation of histone H3 at lysine 4 (H3K4me3) and acetylation of histone H3 at multiple lysine residues (H3Ac) (Liang et al. 2004). Recent evidence suggests that epigenetic control is also involved in the regulation of miRNA gene expression in both normal and cancer cells (Bueno et al. 2008; Kozaki et al. 2008; Lujambio et al. 2008; Vrba et al. 2010).

To more fully understand the role of epigenetic mechanisms in the regulation of normal cell type specific miRNA expression, we studied three different isogenic pairs of human mammary epithelial cells (HMEC) and human mammary fibroblasts (HMF) derived from reduction mammoplasty tissue (Garbe et al. 2009). These normal, previously characterized (Garbe et al. 2009; Novak et al. 2009), finite lifespan cells represent two differentiated cell types typically present within a given organ, each with a distinct phenotype and a distinct epigenotype. The analysis of multiple genotypes allowed us to assess interindividual variability in miRNA expression and epigenetic marks and more precisely identify miRNA genes targeted by epigenetic regulation. To identify cell type specific miRNAs regulated by epigenetic

mechanisms in normal cells, we integrated miRNA expression data obtained by high throughput sequencing of small RNA libraries with the epigenetic profiles of their miRNA promoter regions obtained using a custom designed miRNA tiling microarray. Results from this analysis showed that miRNA gene expression and epigenetic state display high inter-individual concordance within a given cell type; however, inter-cell type concordance was lower, with 13% of expressed miRNAs showing > 10 fold difference in expression between the two normal mammary cell types. We found that a majority of these cell type specific miRNAs are regulated by epigenetic mechanisms in normal cells; 38% were subject to DNA methylation mediated repression of their promoter in the normal non-expressing cells, while 58% were subject to H3K27me3 mediated repression of their promoter in normal non expressing cells. Overall, there is limited overlap of these two repressive marks at individual miRNA promoters, although a few notable exceptions, *MIR10A*, *MIR10B* and *MIR205*, appear to be under dual epigenetic repression by both DNA methylation and H3K27me3 in normal non-expressing cells. In other cases, DNA methylation and H3K27me3 independently target individual miRNA clusters in order to repress complete miRNA families. These results indicate that a significant fraction of cell type specific miRNAs are regulated at the epigenetic level and that these miRNAs are likely to be important targets in human diseases caused by epigenetic dysfunction.

RESULTS

We determined miRNA expression in normal human mammary epithelial and fibroblast cells by high throughput sequencing of small RNA libraries prepared from three isogenic pairs of HMEC and HMF from specimens 48, 184 and 240. About 3.7 million reads in each library were aligned to annotated miRNA regions. Detailed information about sequencing data quality is provided in Supplemental Figures 1-2 and Supplemental Table 1. This miRNA transcriptome sequencing data showed that 392 of 703 (mirbase 13) mature miRNAs were expressed in HMEC and/or HMF at levels that ranged from zero to one million counts per library, demonstrating a large dynamic range of miRNA expression. The expression level of these 392 miRNAs for each of the six samples is provided in Supplemental Data 1. Results also revealed a striking inter-individual concordance in miRNA expression within a cell type, with a correlation of 0.94-0.99 for HMEC and 0.97-0.98 for HMF (Supplemental Figure 3).

Inter-cell type concordance was considerably lower than inter-individual with correlations between HMEC and HMF ranging from 0.75 – 0.84, indicating a substantial population of miRNAs expressed in a cell type selective fashion. Twenty seven percent (104/392) of the expressed miRNAs showed at least 4-fold ($p<0.05$) difference in expression, with 68 showing HMEC selective expression and 36 showing HMF selectivity (Figure 1). Thirteen percent (50/392) of the expressed mature miRNAs showed at least a 10-fold difference in expression between HMEC and HMF. This fraction was considered cell type specific, with 32 miRNAs being HMEC specific and 18 being HMF specific. Figure 2 shows quantitative expression results for several representative cell type specific miRNAs that illustrate the strong inter-individual

concordance in the cell type specific expression as well as the magnitudes of difference that can be seen in miRNA expression between the different cell types (exceeding 3 orders). Examples of mammary epithelial specific miRNAs include miR-205, the two clusters forming the miR-200 family and the miR-183/96/182 cluster (Figure 2, top). The miR-200b/200a/429 cluster of miR-200 family is the only tissue specific cluster that displays substantial variability between individual HMEC genotypes. Mammary fibroblast specific miRNAs are represented by the miR-10 family, the miR-199 family (and miR-214) and the miR-143/145 cluster (Figure 2, bottom). To verify miRNA sequencing data we have analyzed the expression of 10 selected tissue specific miRNAs by real-time PCR (Supplemental Figure 4). The real-time PCR data are in high concordance with miRNA sequencing data, including inter-individual variability of miR-200b. Overall these miRNA expression results indicate that normal human mammary cells show strong cell type specific patterns of a substantial fraction of miRNAs.

Since epigenetic mechanisms play a role in the control of cell type-specific protein coding genes, we performed a broad epigenomic analysis to identify epigenetically regulated miRNA genes. A custom miRNA gene tiling microarray (described in detail in Materials and Methods) was used to probe the epigenetic state of miRNA promoters in each of the three pairs of isogenic HMEC – HMF. 5-methylcytosine or chromatin immunoprecipitated genomic fractions and their respective inputs were hybridized to the microarrays. Then, miRNA targets of DNA methylation, the repressive histone marks H3K27me3 and H3K9me2, and the permissive histone marks of H3Ac and H3K4me3 were identified. The H3K4me3 mark is present on active promoters (Heintzman et al. 2007), reaching a maximum peak at about 500 bp downstream of

the transcription start site (Guenther et al. 2007), and has been extensively used to identify these elements (Marson et al. 2008; Ozsolak et al. 2008). Therefore we used the results from our H3K4me3 analysis to identify and refine the promoter regions of miRNA genes expressed in normal HMEC and HMF (100 or more reads across the libraries). The positions of the identified promoter regions for 169 miRNA genes and gene clusters including 232 miRNA coding regions are provided in Supplemental Data 2, and it is these 169 regions that were evaluated for epigenetic state. These 169 regions include promoters of 24 miRNA gene clusters encoding 37 out of 50 tissue specific miRNAs. The remaining 13 tissue specific miRNAs were either expressed in lower than 100 counts across libraries or there was no significant H3K4me3 enrichment peak in the region covered by microarray and promoter regions were therefore not predicted for these miRNAs.

Figure 3 shows correlations that exist between miRNA expression and the miRNA promoter's epigenetic state. Specifically, either all expressed miRNA genes, or those 10-fold differentially expressed were compared to discover a correlation to the DNA methylation or histone modification state of their respective promoters. The comparisons show that for cell type specific miRNAs there is an increase in correlation between miRNA expression and the various epigenetic marks at their promoter regions. As expected, the correlation was much lower when we analyzed only promoters of miRNAs not differentially expressed (Supplemental Figure 5). With respect to permissive histone marks, H3Ac and H3K4me3 display strong positive correlations with miRNA expression (Figure 3), as well as with each other, consistent with a transcriptionally active state. These permissive histone marks also display strong negative

correlations with DNA methylation and the repressive histone modifications, H3K27me3 and H3K9me2.

Repressive epigenetic marks in miRNA promoter regions show increasingly strong negative correlations as the levels of cell type differential expression increases. In miRNAs that show a >10-fold difference in expression, DNA methylation and H3K27me3 show inverse correlations with miRNA expression of -0.70 and -0.77, respectively, suggesting that a number of these miRNAs are epigenetically regulated (Figure 3). H3K9me2 shows a weaker negative correlation (-0.50) that is more closely associated with DNA methylation than with H3K27me3, supporting the functional linkage between H3K9me2 and DNA methylation (Epsztejn-Litman et al. 2008). While DNA methylation and H3K27me3 both have strong inverse correlations with permissive histone marks and miRNA expression state, these two marks do not correlate well with each other (0.41), supporting their largely independent mechanisms and distinct targets of epigenetic repression. Taken together, these associations suggest a subset of cell type specific miRNA genes are repressed by DNA methylation/H3K9me2 and others by H3K27me3, while only a small fraction of these miRNA genes are likely to be repressed by both epigenetic marks. In addition to promoter regions, we also analyzed the correlation between repressive epigenetic marks and miRNA expression at miRNA hairpin encoding regions downstream of their promoters (Supplemental Figure 6). In these regions H3K27me3 correlates negatively with expression at the level similar to that observed in promoter regions. DNA methylation, however, does not correlate with expression in hairpin coding regions. These results indicate

that DNA methylation plays a promoter-centric repressive role, in contrast to the polycomb specific H3K27me3 that spreads over the whole regions of repressed genes.

We further focused on the promoters of 24 miRNA genes and gene clusters expressing 37 cell type specific miRNAs (Figure 4). Eighteen of these promoters (75%) show cell type specific patterns of DNA or H3K27 methylation that are linked to the transcriptional repression of their associated miRNAs in the non-expressing cell type, while 6 promoters (25%) show no substantial cell type specific differences in repressive epigenetic marks. Nine of 24 promoters (38%) are repressed by DNA methylation, 14 of 24 promoters (58%) are differentially occupied by polycomb specific mark H3K27me3, and interestingly 5 of the 18 epigenetically targeted miRNA promoters possess differences in both, DNA methylation and H3K27me3, suggesting a dual epigenetic repression of these miRNAs. Examples of this small fraction of miRNA genes under dual epigenetic repression by DNA methylation and H3K27me3 include the HMEC-specific *MIR*205 and the HMF-specific *MIR10A* and *MIR10B*.

miR-205 is an HMEC specific miRNA that is functionally related to the miR-200 family. The *MIR205* gene has an increased CpG density at its regulatory region; however, it does not have a CpG island according to the original criteria (Gardiner-Garden and Frommer 1987). H3K4me3 and H3Ac are present in miR-205 expressing HMEC cells, but are absent in non-expressing HMF (Figure 5A). In contrast, the repressive epigenetic marks of DNA methylation, H3K9me2, and H3K27me3 are all present in non-expressing HMF, but are absent in expressing HMEC. To increase the resolution and confirm the DNA methylation data from the microarray analysis, we analyzed certain regions in more detail using MassARRAY technology (Figure 5A, bottom). The

results from MassARRAY are in agreement with the microarray data, showing very low levels of methylation in all HMEC samples and high levels of DNA methylation in HMF. Therefore, in mammary fibroblasts, the *MIR205* gene appears to be under a dual epigenetic repression by both DNA methylation (linked to H3K9me2) and H3K27me3.

A similar dual epigenetic control is seen in the HMF-specific *MIR10A* and *MIR10B* miRNA genes located within the *HOXB* and *HOXD* gene clusters, respectively. In *MIR10A* and *MIR10B* expressing fibroblasts, H3K4me3 and H3Ac are present at *MIR10A* and *MIR10B* promoters, but are absent in non-expressing epithelial cells. In contrast, the repressive H3K27me3 is present throughout the whole region of both the *MIR10A* and *MIR10B* genes in non-expressing HMEC, but is absent in expressing HMF (Figure 5B, Supplemental Figure 7A), consistent with the knowledge that HOX gene clusters are polycomb targets (Simon and Kingston 2009). In addition to the repressive H3K27me3 mark in HMEC, the *MIR10A* and *MIR10B* gene promoters also show HMEC specific DNA methylation (Figure 5B, Supplemental Figure 7A) along with low levels of H3K9me2. These results are similar to those seen for *MIR205*, suggesting that normal cells repress some miRNA genes using multiple epigenetic mechanisms.

Most epigenetically targeted cell type specific miRNAs are repressed in association with either H3K27Me3 or DNA methylation, and these distinct repressive epigenetic states can even be seen in different members of the same miRNA families. One example is the *MIR200* family, an epithelial-specific miRNA family repressed in mesenchymal cells. In this case, both members of the *MIR200* family have their promoter region occupied by H3K4me3 and H3Ac in expressing epithelial cells. In contrast, non-expressing HMF are devoid of these permissive marks and

instead, each member of the *MIR200* family is targeted by different repressive epigenetic marks in these cells. The promoter for the *MIR200B/200A/429* cluster is occupied by H3K27me3, (Figure 5C) indicating that polycomb is responsible for the fibroblast cell type specific repression of this miRNA gene. DNA methylation of the *MIR200B/200A/429* gene has a complex pattern. MassARRAY analysis revealed that the transcription start region located in the distal part of the CpG island is unmethylated in HMEC and has a low level of methylation in HMF (Figure 5C). The other analyzed regions downstream of the TSS, however, show that DNA methylation alternates between non-expressing and expressing cells in this particular H3K27me3 target gene (Figure 5C). The proximal part of the CpG island shows more DNA methylation in expressing HMEC samples. Then follows the region methylated more in non-expressing fibroblasts and finally, the area just upstream the *MIR200B* hairpin coding region shows an intermediate level of methylation in both cell types. Therefore DNA methylation does not seem to play any conclusive role in normal tissue specific repression of *MIR200B/200A/429* cluster. In contrast to the *MIR200B/200A/429* cluster, we have previously shown DNA methylation and H3K9Me2 to be important in the repression of the *MIR200C/141* members of the family (Vrba et al. 2010), and these earlier observations are further confirmed by the microarray analysis in the present studies (Figure 5D). The DNA of the whole *MIR200C/141* region is unmethylated in expressing HMEC and the microarray data show that DNA methylation in HMF reaches a maximum in the region just downstream the TSS. The lack of H3K27me3 enrichment in *MIR200C/141* region in both mammary cell types indicates that this important cell type specific miRNA cluster is not a polycomb target. Since both clusters of the *MIR200* family share a high level of expression in epithelial cells, but no expression in

fibroblasts, the distinct repressive epigenetic marks observed for the members of the *MIR200* family suggest that distinct epigenetic mechanisms are involved in their respective repression.

Similar multifaceted forms of epigenetic repression of miRNA families are seen in the fibroblast specific *MIR199* family, whose members consist of the *MIR199A2/214* cluster, *MIR199A1* and *MIR199B*. These three miRNA genes of the *MIR199* family are located at homologous positions on the antisense strands of introns of the three members of the *DNM* gene family. The *MIR199A2/214* cluster is located in *DNM3*, *MIR199A1* in *DNM2* and *MIR199B* in *DNM1*, indicating co-evolution of the *MIR199* family together with the *DNM* gene family. Similar to HMEC specific miRNA genes *MIR200C/141* and *MIR205*, there is an increased CpG density in the promoters of the *MIR199* genes; however, it does not meet the original CpG island definition criteria. The miRNA promoters are occupied by H3K4me3 and H3Ac in expressing fibroblasts, but these marks are absent in epithelial cells. Instead, in non-expressing epithelial cells the *MIR199A2/214* cluster is DNA methylated and H3K9me2 is present, but significant levels of H3K27me3 were not detected, indicating that this region is not a polycomb target (Figure 5E). In contrast, only DNA methylation-linked repression was detected in the *MIR199A1* regulatory region in epithelial cells, (Supplemental Figure 7B) while *MIR199B* utilizes a dual epigenetic repression, that of DNA methylation in combination with H3K27me3 (Supplemental Figure 7C). Overall, these results suggest that expression of the three members of the fibroblast specific *MIR199* family is repressed predominantly by DNA methylation and to a lesser extent by H3K27me3.

A surprising cell type specific miRNA gene with respect to repressive epigenetic marks is the *MIR183/96/182* gene. The entire *MIR183/96/182* region is heavily occupied by H3K27me3 in non-expressing HMF, but H3K27me3 is absent in expressing HMEC (Figure 5F), suggesting that the polycomb repression is the critical repressive epigenetic mechanism regulating the *MIR183/96/182* cluster gene. DNA methylation shows an unexpected phenomenon in this region. Although the TSS region is DNA methylation free for both cell types, downstream of the TSS at the proximal end of the CpG island there exists a differentially methylated region that is DNA methylation free in all three non-expressing HMF samples and heavily methylated in all three expressing HMEC samples (Figure 5F). MassARRAY analysis confirmed the microarray data for all three genotypes. Thus the *MIR183/96/182* cluster is a cell type specific miRNA gene repressed by polycomb, where DNA methylation within the promoter region inversely correlates with H3K27me3 and positively correlates with expression (Figure 4). Since the DNA hypermethylation in HMEC is located downstream of the TSS, in the area that is most occupied by polycomb specific mark H3K27me3 in non-expressing HMF (Figure 5F), it may represent a case of antagonism between DNA methylation and polycomb repression as was recently described in a mouse model (Wu et al. 2010).

Taken together our data show strong tissue specific expression of substantial fraction of miRNAs between mammary epithelial cells and mammary fibroblasts, exceeding three orders of magnitude for some miRNAs. Most of the promoters of these tissue specific miRNA genes are occupied by H3K27me3 or DNA methylation or both of these marks in non-expressing cells

indicating that epigenetic state of miRNA promoters plays an important role in the cell type specific control of miRNA expression.

DISCUSSION

In this study, we sought to identify cell type specific miRNAs regulated by epigenetic mechanisms. To this end, we analyzed the expression levels and the epigenetic state of miRNA genes in three isogenic pairs of normal, finite lifespan HMEC and HMF – two predominant differentiated cell types of ectodermal and mesodermal origin, respectively, found in mammary tissue. miRNA expression and epigenetic state showed strong interindividual concordance within a given cell type, but significant expression and epigenetic differences were found between the different cell types. We found 13% of expressed miRNAs to be expressed in a cell type specific fashion (>10 fold difference between the two cell types), including several known to be important for maintaining cell specific phenotypes. The differential expression of a majority of these cell type specific miRNAs was linked to cell type specific differences in the epigenetic state of their promoters indicating that epigenetic mechanisms play an important role in the regulation of cell type specific miRNA genes.

To identify miRNA promoters utilized by HMEC and HMF (Supplemental Data 2), we used H3K4me3 ChIP-chip data that we obtained from these cells, since this mark is exclusively present at promoters (Heintzman et al. 2007). We used the complementary miRNA expression

data obtained from these same cells to limit promoter identification to only those miRNA expressed in at least one of the mammary cell types, allowing for precise identification of miRNA promoters relevant to human mammary cells. Our results revealed that the promoters of cell type specific miRNAs mostly lacked H3K4me3 enrichment in the inactive promoters of the non-expressing cell type (Figure 5A, C-E), suggesting that these represent the epigenetically labile miRNAs of normal, non-diseased cells. Similar results were reported previously for tissue specific protein coding genes (Guenther et al. 2007). Finally, the H3K4me3 ChIP-chip results further suggest that H3K4me3-directed prediction of promoters for miRNA genes, and likely all genes in general, will be the most accurate if derived from cells known to express the genes of interest.

Of the 24 cell type specific miRNA genes, three quarters (75%) were found to be repressed by H3K27me3 or DNA methylation in the non-expressing cell type, with 58% of cell type specific promoters differentially occupied by H3K27me3, 38% differentially occupied by DNA methylation, and 21% differentially occupied by both H3K27me3 and DNA methylation. In miRNAs repressed by H3K27me3, we find this mark extends beyond the promoter and encompasses larger regions that include the miRNA gene body, consistent with recent findings demonstrating a spreading of the H3K27me3 mark from the promoter during differentiation of human embryonic stem cells (Hawkins et al. 2010). Interestingly, when we extend our analysis beyond only miRNA promoters differentially active in mammary cells by integrating our H3K27me3 ChIP-chip data with all the predicted miRNA promoter data and known miRNA hairpin coding regions, we found that approximately 27% of all miRNA promoters as well as

miRNA hairpin coding regions are enriched for H3K27me3 (Supplemental Figure 8). In contrast, it has been estimated that only 9% of promoters of protein-coding genes are occupied by H3K27me3 (Bracken et al. 2006). Thus, H3K27me3, a polycomb mark responsible for regulating genes involved in cell identity and differentiation, shows an approximately 3-fold bias towards miRNA compared to protein-coding genes, providing further support for an important role for miRNAs as regulators of cell fate and phenotype and H3K27me3 as an important regulator of cell type specific miRNA expression.

Cell type-specific DNA methylation of miRNA promoters was correlated with the presence of the H3K9me2 mark and the repression of the associated miRNAs, further supporting the functional linkage between these two repressive epigenetic marks (Epsztejn-Litman et al. 2008). The DNA methylation mark was found to be centered on the promoter regions of the miRNA and did not extend far upstream or downstream, in contrast to what was observed with the H3K27me3 repressive mark. In addition, a common feature of DNA methylation repressed miRNA genes was the absence of a CpG island in the promoter region; in the case of cell type specific miRNA genes with CpG island promoters, the H3K27me3 mark is most often responsible for transcriptional repression (Figure 5A-F).

The weakest correlation between epigenetic marks was between DNA methylation/H3K9me2 and H3K27me3. The limited overlap between DNA methylation/H3K9me2 and H3K27me3 in miRNA promoters likely reflects the largely independent nature of these two epigenetic repressive pathways in normal cells. Despite this limited overlap there are miRNAs where both marks appear to be involved in their cell type

specific repression. The coincidence of DNA methylation and H3K27me3 on the same miRNA promoters may represent mutual fail-safe mechanisms so that disruption of one epigenetic mechanism is not sufficient to initiate aberrant activation of the miRNA. If this is the case, then miRNA targets of this dual epigenetic repression may be critical to maintain cell integrity/identity, and their compromise could be involved in the genesis of human disease states, including cancer. Two examples of miRNAs that support the possible importance of dual epigenetic repression are miR-205 and miR-10a and miR-10b, since their dysregulation has already been linked to a variety of different cancers (Gregory et al. 2008b; Ma and Weinberg 2008; Greene et al. 2010; Lund 2010). For example, the loss of epithelial-specific miR-205 in cancers of epithelial origin has been linked to the acquisition of aggressive tumor phenotypes (Baffa et al. 2009; Iorio et al. 2009; Tellez et al. 2011), while gain of expression of fibroblast-specific miR-10 family members by cancers of epithelial origin have similarly been linked to aggressive tumor phenotypes (Ma et al. 2007; Baffa et al. 2009; Tian et al. 2010).

miR-205 participates in the maintenance of the epithelial phenotype, is expressed in epithelial cells but not in fibroblasts, and is related to the miR-200 family (Gregory et al. 2008a; Park et al. 2008). Expression of miR-205 and the miR-200 family members appears incompatible with a mesenchymal phenotype, and since miR-205 is expressed at much higher levels than the miR-200 family members in HMEC, it is possible that dual epigenetic repression by DNA methylation and H3K27me3 in fibroblasts is necessary to prevent any inappropriate miR-205 expression. miR-205 along with the miR-200 family target the mesenchymal specific transcriptional repressors *ZEB1* and *ZEB2* (Gregory et al. 2008a). Possibly the total level of the

miR-200 family and miR-205 secures an epithelial phenotype, and complete epigenetic silencing of *MIR205* is necessary to allow *ZEB1* and *ZEB2* to be expressed at levels sufficient to direct the mesenchymal phenotype.

Similar to *MIR205*, we have found that the closely related *MIR200* family members are also epigenetically regulated in a cell type specific fashion. We and others have previously shown that the *MIR200* family members *MIR200C/141* have a permissive epigenetic state in expressing epithelial cells, while non-expressing fibroblasts display a repressed epigenetic state driven by DNA methylation and H3K9me2, but not H3K27me3 (Vrba et al. 2010). In contrast, the fibroblast specific repression of the other *MIR200* family members *MIR200B/200A/429* is linked to the H3K27me3 mark, and DNA methylation and H3K9me2 do not appear to play a decisive role in its repression (Figure 5C). Therefore, the two genes of the *MIR200* family that likely arose from a single common ancestor, have acquired different mechanisms of epigenetic regulation during evolution. Overall, these results suggest that complete epigenetic transcriptional repression of individual miRNAs may require complementary epigenetic mechanisms to prevent spurious transcriptional activity. Similarly, our results also suggest that complementary epigenetic repressive mechanisms may act independently to repress distinct members of the same miRNA family, as is the case with the *MIR200* family.

miR-10a and miR-10b are expressed in a fibroblast specific fashion and appear to be under dual epigenetic repression in the epithelial cells. Both *MIR10A* and *MIR10B* show significant H3K27me3 and DNA methylation in their promoter regions and both are found in HOX gene clusters, gene families well known for rich and complex epigenetic regulation in normal and

cancer cells (Rauch et al. 2007). Interestingly miR-10b has been reported to be aberrantly expressed in breast cancer cells and this expression is linked to an aggressive cancer phenotype (Ma et al. 2007; Baffa et al. 2009), although this conclusion has been questioned based on the analysis of primary breast cancer specimens which showed no correlation between miR-10b expression levels and clinical progression (Gee et al. 2008). Several molecular, cellular, and organismal facets may contribute to these two different conclusions. The data presented in this study strongly suggests that epigenetic control of cell type specific expression is one important facet. The experimental biological studies used pure cancer cell line populations to first detect and then verify miR-10b's phenotypic effects. In contrast, it appears that the analysis of breast cancer clinical specimens was performed on heterogeneous tissue samples. Detecting aberrant expression of miR-10b in breast tumor cells from a complex tissue specimen is likely to be difficult, since mammary fibroblasts can constitute a significant portion of stromal cell content typically found in such specimens, and they express >3 orders of magnitude higher levels of miR-10b compared to mammary epithelial cells. This very high expression of miR-10b in the stromal cells of the tissue specimens could obscure any significant changes within the breast cancer cells themselves.

Indeed, this cautionary note extends to all the cell type specific miRNAs identified in this study. The large magnitude differences seen in the expression levels and epigenetic states of these miRNAs between HMEC and HMF limit the ability to easily determine over- or under-expression or epigenetic status from the analysis of heterogenous tissue samples. Precise analysis of these miRNAs will require approaches that assess the expression or epigenetic state

of these miRNAs in specific cell types within a tissue specimen. This is especially important since many of the epigenetically regulated cell type specific miRNAs identified in this study have already been associated with or functionally linked to human carcinogenesis. The tissue specific miRNAs that have been found deregulated in cancer are summarized in Supplemental Table 2.

In summary, our study has revealed a significant level of cell type specific miRNA expression associated with human mammary epithelial and fibroblast cells. We also showed that epigenetic modifications play an important role in this cell type specific miRNA regulation. The two epigenetic pathways responsible for deployment of repressive epigenetic marks - DNA methylation and H3K27me3 act largely independently. H3K27me3, a hallmark of polycomb repression, appears to play the major role in the normal cell type specific repression of miRNA genes. Examples of polycomb targets are the *MIR200B/200A/429* and *MIR183/96/182* genes. Some highly cell type specific miRNA genes like *MIR200C/141* and *MIR199A2/214*, however, are not polycomb targets and their differential expression is determined predominantly by cell type specific DNA methylation at the promoter region, often in collaboration with the H3K9me2 histone mark in non-expressing cells. A common feature of these miRNA genes repressed by DNA methylation is the lack of CpG islands. Different genes forming miRNA families are repressed by different epigenetic marks, indicating that they are targeted by different epigenetic mechanisms. Some miRNA genes, including *MIR205*, *MIR10A* and *MIR10B*, are under dual epigenetic repression by both DNA methylation and H3K27me3. The miRNAs found to be cell type specific and repressed by epigenetic marks in non-expressing cells are often

deregulated in cancer, indicating that the disruption of normal epigenetic regulation of cell type specific miRNA expression can be involved in carcinogenesis. Knowing which epigenetic marks are involved in repression of individual miRNA genes in normal cells and the locations of relevant regulatory regions thus contributes to our better understanding of these processes.

METHODS

Cell lines and cell culture

Finite lifespan pre-stasis HMEC from specimens 184 (batch D), 48 (batch RT), and 240L (batch B), were derived from reduction mammoplasty tissue of women aged 21, 16, and 19 respectively (Garbe et al. 2009). Cells were initiated as organoids in primary culture in serum-containing M85 medium supplemented with oxytocin (Bachem) at 0.1 nM , and maintained in M87A medium supplemented with oxytocin and cholera toxin at 0.5 ng/ml (Garbe et al. 2009). Fibroblasts from specimens 184, 48, and 240L were obtained by growing primary reduction mammoplasty cells in DMEM/F12 with 10% FBS and 10 µg/ml insulin and further propagated in DMEM/F12 with 10% FBS, as previously described (Garbe et al. 2009). The cells used in this study were within cell culture passages 4-9 from primary tissue. Our previous study shows that these cells do not acquire epigenetic changes as late as passage 14. It is only following the emergence from the stasis proliferation barrier (Garbe et al. 2009) that HMEC first show the acquisition of significant epigenetic changes (Novak et al. 2009).

Small RNA library preparation and sequencing

Total RNA from epithelial cells or fibroblasts was extracted using the Trizol method (Invitrogen, Carlsbad, CA, USA). The small RNA fraction (18-35 nt) was purified on 15% denaturing polyacrylamide gel. A preadenylated adaptor (rAppCTGTAGGCACCATCAAT3ddC) was ligated to the 3' end of small RNA using truncated T4 RNA ligase 2 (New England Biolabs, Ipswich, MA, USA), followed by purification of the ligation product on 15% denaturing polyacrylamide gel. A Illumina specific 5' adaptor (GTTCAGAGTTCTACAGTCCGAcgauc –upper case DNA, lowercase RNA) was ligated using T4 RNA ligase 1 (New England Biolabs) and the product was purified on a 10% denaturing polyacrylamide gel. Small RNAs with ligated adaptors were reverse transcribed into DNA using Superscript III reverse transcriptase (Invitrogen) and a primer with a Illumina specific extension on its 5' end (GACATCCGTGGTAGTTAGCATACGGCAGAAGACGAAC). The cDNA was then amplified by 15 cycles of PCR using Phusion DNA polymerase (Finnzymes, Woburn, MA, USA) and Illumina specific primers (AATGATACGGCGACCACCGACAGGTTCAGAGTTCTACAGTCCGA and GACATCCGTGGTAGTTAGCATACGGCAGAAGACGAAC). The resulting ~110 bp PCR products were separated and purified from a 3% agarose gel, and submitted for Illumina sequencing to NCGR, Santa Fe, NM, USA. The data were deposited in SRA archive, accession no SRP001530.1.

Data analysis

Results from the Illumina Genome Analyzer were received in the fastq format. The reads were mapped to the hg18 human genome assembly using the program Novoalign (www.novocraft.com). Output from Novoalign was further analyzed in R

(R_Development_Core_Team 2011). First, data were converted to bed format and peaks of reads were found for pooled data from all samples. The peak regions were used for counts and annotation of reads in individual samples. Counts were normalized for the total number of reads in individual libraries (see Filtered reads in Supplementary table 1). The miRNAs with at least 10 reads across the libraries represented in at least two libraries were considered expressed and further analyzed. Package edgeR was used for the differential expression calculation.

miRNA gene tiling microarray design

Human miRNA coding sequence positions were downloaded from the miRNA database (ver 13) (http://microrna.sanger.ac.uk/sequences/). This dataset contains information about the positions of 718 miRNA coding regions in the human genome. 454 out of 718 miRNA coding regions have their promoter predicted (Marson et al. 2008). Another 149 of miRNA coding regions are part of known protein coding genes. For these miRNAs the TSS of the host gene was assumed as TSS for miRNA and the position of this region was obtained as the 5' end of the known gene from the UCSC genome browser. The entire region from 10 kb upstream of the predicted promoter (TSS) region down to 5 kb downstream of the miRNA hairpin coding region was tiled for all these 603 miRNA coding regions. For the remaining 115 miRNA coding regions, where there was no prediction of TSS nor do they lie within protein coding genes, the whole region from 70 kb upstream of the hairpin coding region down to 5 kb downstream was tiled. Additionally about 100 protein coding genes including controls like GAPDH and ACTB were added. The probes used to tile the specified regions were from the Agilent whole genome tiling

microarray set and the Agilent promoter 2 microarray set. The resulting number of probes totals over 99,000, with approximately 5 probes per kbp. The microarrays were manufactured by Agilent (Agilent Technologies, Santa Clara, CA, USA) using their 2 x 105 k platform. Agilent design ID is 024305.

Methyl cytosine DNA and chromatin immunoprecipitation

Methyl cytosine DNA immunoprecipitation (MeDIP) was performed using 5-methylcytosine specific monoclonal antibody as described (Weber et al. 2005).

Chromatin immoprecipitation (ChIP) was performed as described previously (Oshiro et al. 2003; Vrba et al. 2008) using antibodies specific for histone H3 trimethylated at lysine 4 (#05-745, Upstate), histone H3 trimethylated at lysine 27 (#07-449, Millipore), acetylated histone H3 (#06-599, Millipore), and histone H3 dimethylated at lysine 9 (CS200587, Millipore).

Sample labeling and microarray hybridization

MeDIP DNA or ChIP DNA samples were amplified using the random primed approach and 2 ug of amplified DNA was labeled as described (Vrba et al. 2008). Cy5 was used for input samples, Cy3 for immunoprecipitated samples. After labeling and purification, Cy3 and Cy5 labeled samples were pooled and vacuum concentrated to a volume of 91.5 µl. Twelve and halve µl of human Cot-1 DNA (1µg/µl, Invitrogen Cat. No. 15279-011), 26 µl of Agilent blocking agent (10x) and 130 µl of Agilent hybridization buffer (2x) were added. Samples were heated for 3 min at 95 ^{o}C, transferred to 37 ^{o}C, incubated for 30 min, and then used for microarray hybridization for 28h at 65 ^{o}C. After hybridization, slides were washed in Agilent Oligo aCGH/ChIP-on-Chip Wash Buffer 1 for 5 min at room temperature, then in Agilent Oligo

aCGH/ChIP-on-Chip Wash Buffer 2 for 5 min at 37 ^{o}C, washed in acetronitrile for 10 s at room temperature and finally in stabilization and drying solution for 30 s at room temperature. The scanning was performed using an Axon GenePix 4000B microarray scanner (Axon Instruments, Inc., Foster City, CA, USA) and GenePix 6.0 software at 5 µm resolution and PMT settings 750 (635nm) and 600 (532nm).

Microarray data analysis

Output from GenePix (*.gpr files) were imported to R using the limma package. Individual channels were first spatially normalized within arrays using ma2D function from the package marray and then loess normalized between arrays using the function normalize.loess from package affy. The RG object was transformed to an MA object and M values were again loess normalized between arrays. M values (log2 ratios of input to immunoprecipitated channel) were used for further analysis as a measure of enrichment of a region centered on individual probes. Differences in histone modification were determined in 2 kb region centered on TSS region or miRNA hairpin region. The paired t-test was used to analyze data from all probes in each 2 kb region. Differentially enriched regions were defined as regions where the average difference of ratio was at least 1.5 fold and the p-value ≤ 0.05.

Transcription start regions prediction

We predicted miRNA TSS regions based on the fact that H3K4me3 is present in TSS regions, reaching maximum enrichment at about 0.5 kb downstream TSS (Guenther et al. 2007). To reduce the amount of false predictions we used the most proximal major peak of H3K4me3 enrichment, upstream of the miRNA hairpin region which was at least 2 fold enriched over

input. Further we limited the predictions only for miRNAs that are expressed (at least 100 reads in libraries). For differentially expressed miRNAs the pooled H3K4me3 data from expressing samples (either HMEC or HMF) were used, for other miRNAs the pooled H3K4me3 data from all 6 samples were used. Once the peak of H3K4me3 enrichment was identified, the area between the peak and nearby Switch gear TSS or EST 5' end was considered TSS region. Switch gear TSS and EST positions were downloaded from UCSC browser. For miRNAs where there was no Switch gear TSS or EST end in the vicinity (2.5 kb upstream 0.5 kb downstream) of the H3K4me3 peak, the region from H3K4me3 peak 1 kb upstream was considered TSS region.

DNA methylation analysis by MassARRAY

DNA methylation analysis by MassARRAY was performed as described (Novak et al. 2009). Primer sequences are listed in Supplemental Table 3.

All oligonucleotides used in this study were ordered from Integrated DNA Technologies (Coralville, IA, USA).

DATA ACCESS

The sequence data from this study have been submitted to NCBI Sequence Read Archive (http://www.ncbi.nlm.nih.gov/sra) under accession no. SRP001530.1. The microarray data have been submitted to GEO database, accession no. GSE28380.

ACKNOWLEDGMENTS

This work was supported by grants CA-65662, 1U01CA153086-01 and by Margaret E and Fenton L Maynard Endowment for Breast Cancer Research. J.C.G. and M.R.S. were supported by Department of Defense grant BCRP BC060444 (JG, MS) carried out at Lawrence Berkeley National Laboratory under Contract No. DE-AC02-05CH11231.

.

FIGURE LEGENDS

Figure 1. Differential miRNA expression between HMEC and HMF obtained from three independent pairs of samples. The y-axis displays the HMEC to HMF expression ratio, the x-axis displays the average expression of miRNAs, both axis are in logarithmic scale. Differentially expressed miRNAs (at least 4 fold difference in expression, p-value ≤ 0.05) are highlighted in red color. The blue dashed horizontal lines indicate 10 fold differences in expression. Several cell type specific miRNAs are marked.

Figure 2. Expression data for selected cell type specific miRNA genes obtained by sequencing of small RNA libraries from isogenic pairs of human mammary epithelial and fibroblast cells. Displayed are the normalized counts for each sample. The individual HMEC samples are in green, their paired HMF samples are in red. The expression levels of the 392 detected mature miRNAs across all six samples are presented in Supplemental Data 1.

Figure 3. Differences in HMEC/HMF miRNA expression correlated with differences in epigenetic marks at their promoters. We used data from all probes within a 2 kb region centered on the predicted TSS region and calculated the correlation of difference in enrichment of individual epigenetic marks between the cell types. The left panel shows correlations for all 169 miRNA genes and gene clusters, where the promoter was predicted and the right panel shows 24 cell

type specific miRNA genes only. The numbers show correlation coefficients for individual pairs of epigenetic marks.

Figure 4. Cell type specific miRNA genes (clusters), their difference in expression and differences in occupation of their promoter regions by 5 epigenetic marks. The data are presented as log2(fold difference HMEC/HMF). The color scale indicates whether the data behave as expected for HMEC specific miRNAs (green) or HMF specific miRNAs (red). The *MIR424~450B* is label for the *MIR424/503/542/450A2/450A1/450B* cluster.

Figure 5. The epigenetic state of cell type specific miRNA genes in HMEC and HMF. Top part shows the enrichment of individual epigenetic marks through the regions in a heatmap form, with yellow indicating no enrichment and blue color indicating high enrichment. The data for HMEC and HMF samples are averages from three genotypes of HMEC and HMF respectively. The chromosomal positions are according to the hg18 human genome assembly. The miRNA hairpin coding regions are displayed as a red rectangles and predicted transcription start site regions as brown triangles. Small black rectangles at the top lane indicate positions of individual microarray probes. The tics at the bottom indicate positions of individual CpG dinucleotides. CpG islands according to UCSC are displayed as green rectangles when present. The blue rectangles at the bottom lane indicate positions of regions analyzed for DNA methylation by MassARRAY technology. Results from MassARRAY for individual regions indicated are shown at the bottom part. The level of methylation of individual CpG units within

the MassARRAY amplicon is displayed as a heatmap with the lowest methylation (0%) in yellow and the highest methylation (100%) in blue. The individual samples are labeled on the left side. The individual CpG units are marked at the bottom.

FIGURES

Figure 1

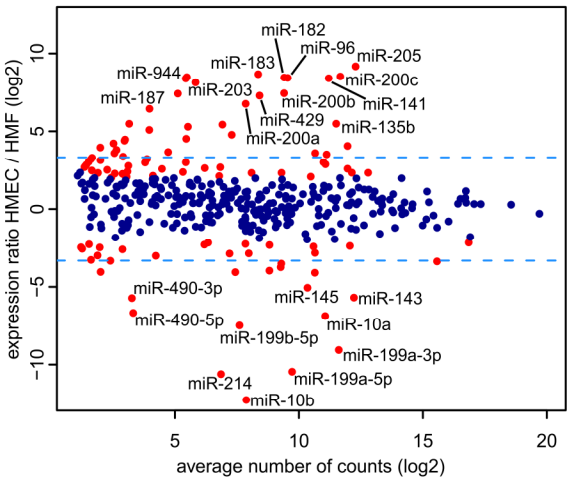

Figure 2

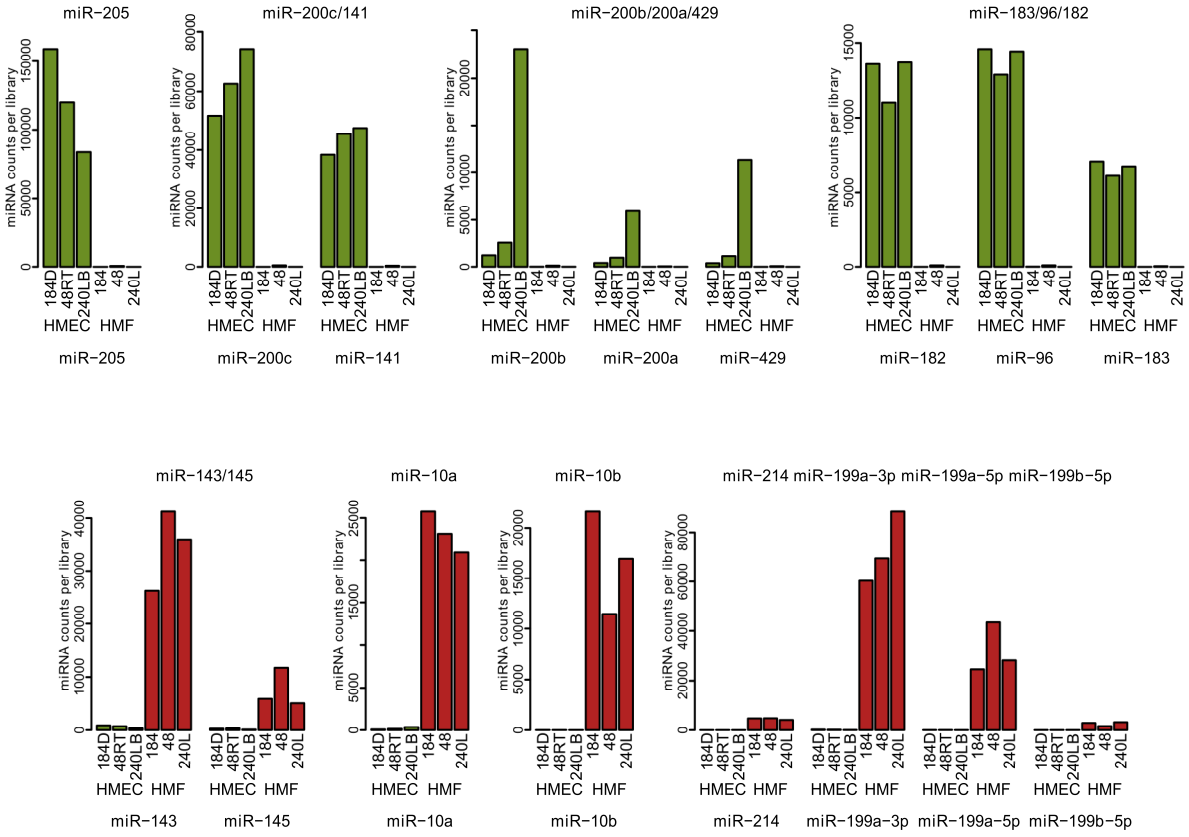
miR−205
miR−200c/141
miR−200b/200a/429
miR−183/96/182
miR−143/145
miR−10a
miR−10b
miR−214 miR−199a−3p miR−199a−5p miR−199b−5p
miRNA counts per library
184D
48RT
240LB
184
48
240L
HMEC
HMF
miR−205
miR−200c
miR−141
miR−200b
miR−200a
miR−429
miR−182
miR−96
miR−183
miR−143
miR−145
miR−10a
miR−10b
miR−214
miR−199a−3p
miR−199a−5p
miR−199b−5p

Figure 3

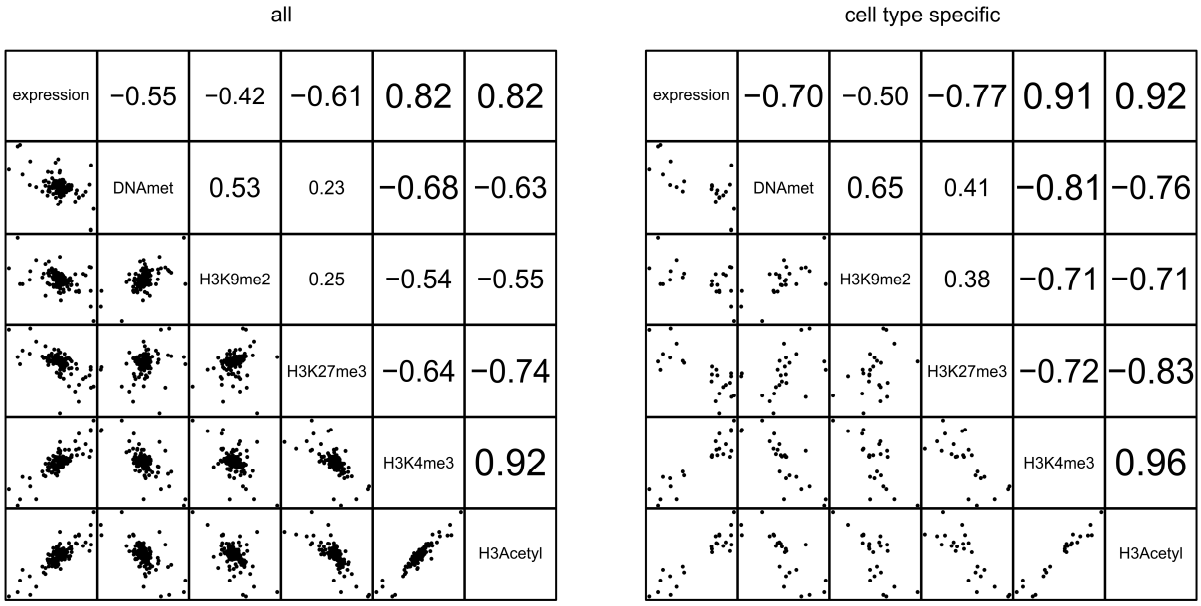
all
expression
−0.55
−0.42
−0.61
0.82
0.82
DNAmet
0.53
0.23
−0.68
−0.63
H3K9me2
0.25
−0.54
−0.55
H3K27me3
−0.64
−0.74
H3K4me3
0.92
H3Acetyl
cell type specific
expression
−0.70
−0.50
−0.77
0.91
0.92
DNAmet
0.65
0.41
−0.81
−0.76
H3K9me2
0.38
−0.71
−0.71
H3K27me3
−0.72
−0.83
H3K4me3
0.96
H3Acetyl

Figure 4

cluster ID	expression	DNAmet	H3K9me2	H3K27me3	H3K4me3	H3Acetyl
MIR205	9.17	−1.14	−1.23	−1.68	3.16	3.26
MIR183/96/182	8.52	1.17	0.29	−1.76	0.71	0.84
MIR944	8.46	−2.25	−0.81	−0.50	2.29	2.32
MIR200C/141	8.46	−2.22	−0.38	−0.32	2.40	1.56
MIR203	8.15	0.14	0.31	−0.90	0.21	0.34
MIR200B/200A/429	7.15	−0.23	0.07	−1.02	1.23	1.02
MIR187	6.49	−0.41	0.11	−1.15	0.44	0.74
MIR135B	5.49	−0.51	−0.41	−1.55	2.08	1.54
MIR582	5.46	−0.54	−0.37	−2.79	0.87	1.61
MIR1910	4.98	−0.15	−0.21	−0.44	0.35	0.90
MIR584	4.74	−0.32	−0.40	−0.10	0.79	0.96
MIR577	4.56	−0.74	0.10	−2.04	1.46	1.47
MIR147B	3.63	0.06	−0.10	0.10	0.35	0.25
MIR210	3.59	0.11	−0.21	−0.38	0.21	0.51
MIR378	3.50	−0.09	−0.22	−0.81	0.25	0.69
MIR424~450B	−3.45	0.31	0.12	0.33	−1.28	−1.31
MIR497/195	−3.80	−0.21	0.01	0.45	−0.97	−0.85
MIR143/145	−5.37	0.02	0.50	1.51	−3.17	−2.42
MIR10A	−6.86	1.37	0.19	2.41	−2.15	−3.03
MIR490	−7.00	0.12	−0.06	0.65	−1.51	−1.60
MIR199B	−8.82	0.67	−0.19	0.87	−1.40	−1.10
MIR199A1	−9.47	2.23	−0.19	−0.11	−3.17	−1.93
MIR199A2/214	−10.07	2.15	1.15	0.41	−3.67	−2.82
MIR10B	−12.29	0.94	0.27	2.33	−2.38	−3.15

Figure 5

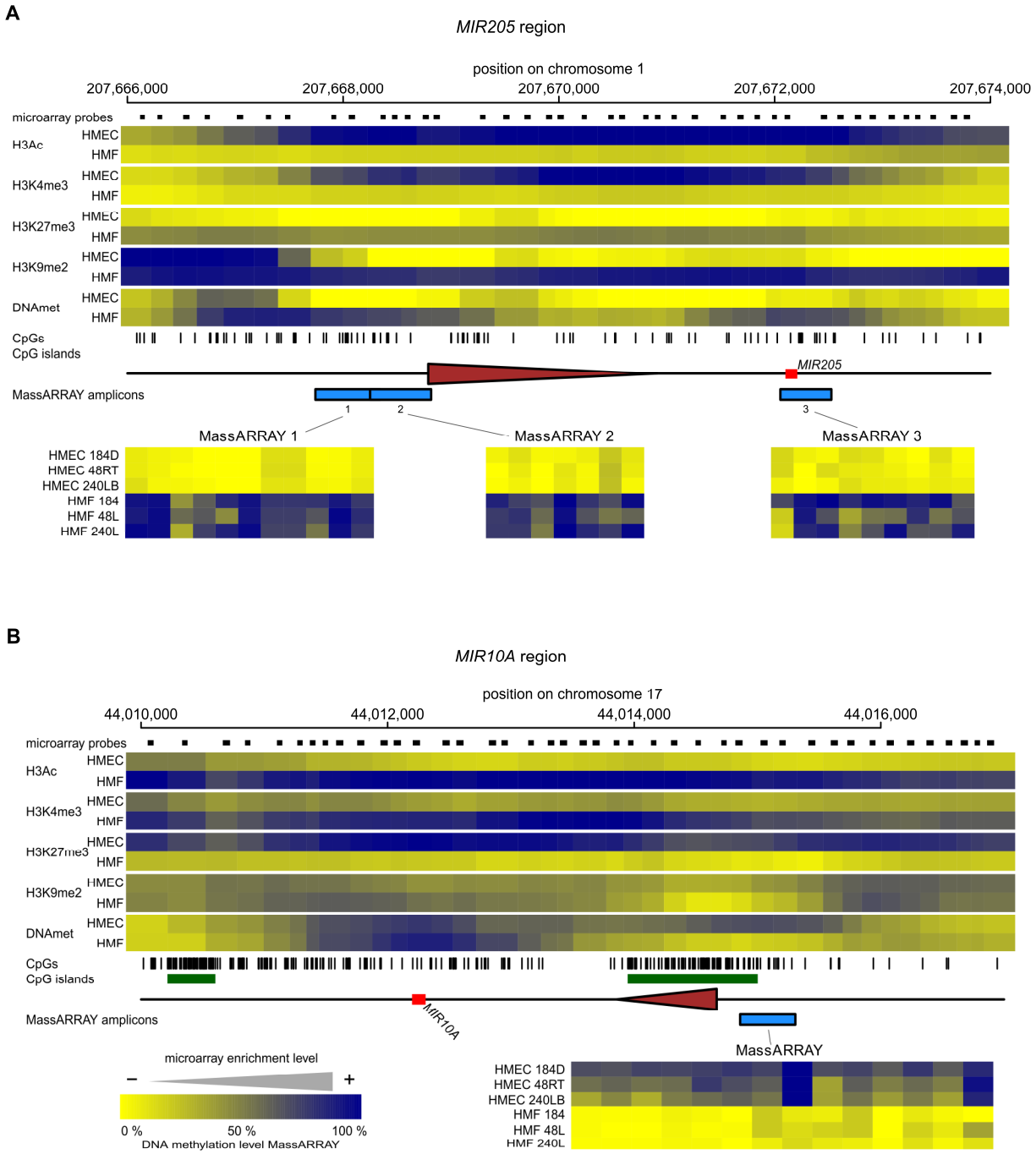
A
MIR205 region
position on chromosome 1
207,666,000
207,668,000
207,670,000
207,672,000
207,674,000
microarray probes
H3Ac
HMEC
HMF
H3K4me3
H3K27me3
H3K9me2
DNAmet
CpGs
CpG islands
MIR205
MassARRAY amplicons
1
2
3
MassARRAY 1
MassARRAY 2
MassARRAY 3
HMEC 184D
HMEC 48RT
HMEC 240LB
HMF 184
HMF 48L
HMF 240L
B
MIR10A region
position on chromosome 17
44,010,000
44,012,000
44,014,000
44,016,000
microarray probes
H3Ac
HMEC
HMF
H3K4me3
H3K27me3
H3K9me2
DNAmet
CpGs
CpG islands
MassARRAY amplicons
MIR10A
MassARRAY
microarray enrichment level
–
+
0 %
50 %
100 %
DNA methylation level MassARRAY
HMEC 184D
HMEC 48RT
HMEC 240LB
HMF 184
HMF 48L
HMF 240L

Figure 5

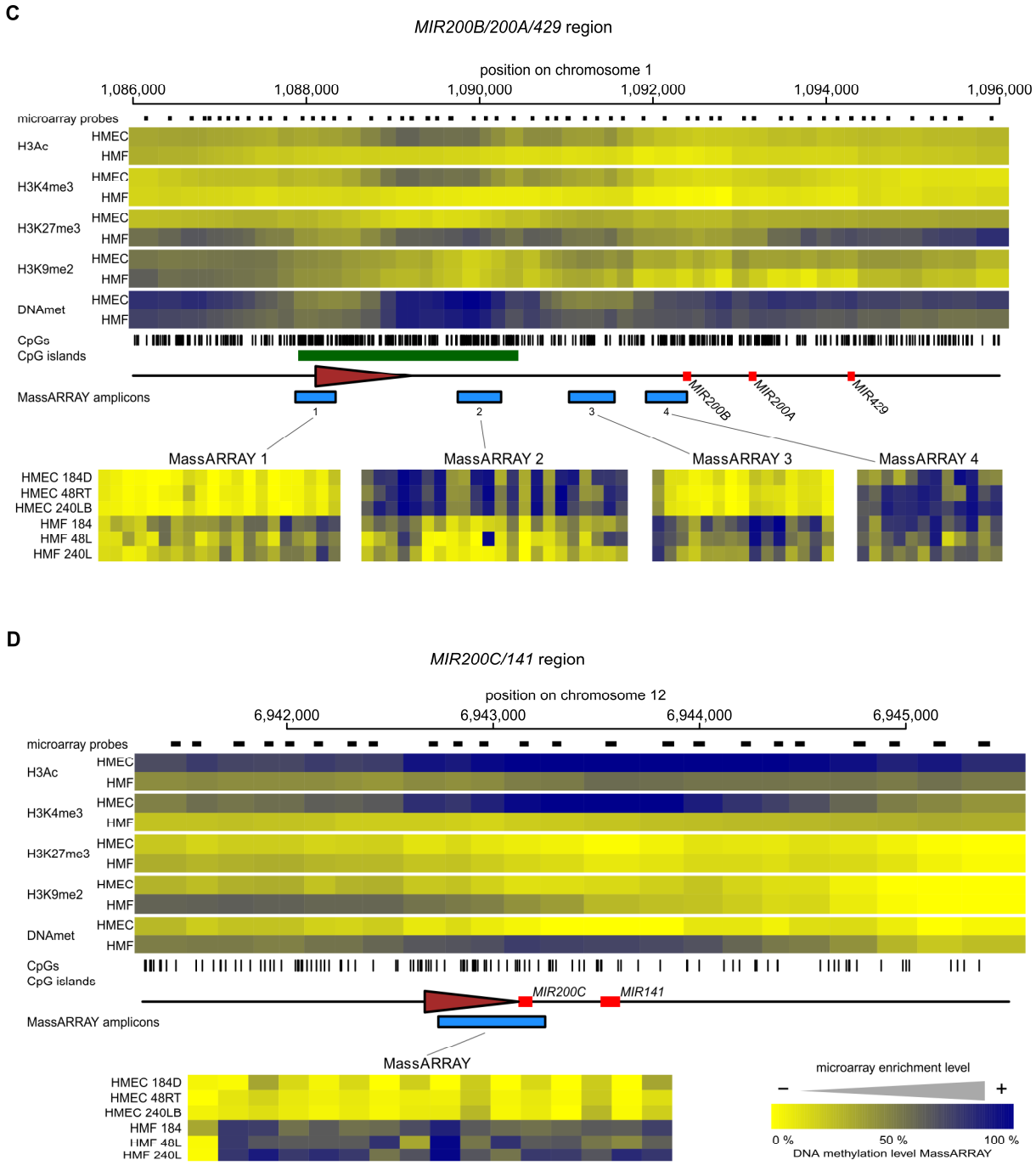
C
MIR200B/200A/429 region
position on chromosome 1
1,086,000
1,088,000
1,090,000
1,092,000
1,094,000
1,096,000
microarray probes
H3Ac
H3K4me3
H3K27me3
H3K9me2
DNAmet
HMEC
HMF
CpGs
CpG islands
MassARRAY amplicons
MIR200B
MIR200A
MIR429
MassARRAY 1
MassARRAY 2
MassARRAY 3
MassARRAY 4
HMEC 184D
HMEC 48RT
HMEC 240LB
HMF 184
HMF 48L
HMF 240L
D
MIR200C/141 region
position on chromosome 12
6,942,000
6,943,000
6,944,000
6,945,000
MIR200C
MIR141
MassARRAY
microarray enrichment level
0 %
50 %
100 %
DNA methylation level MassARRAY

Figure 5

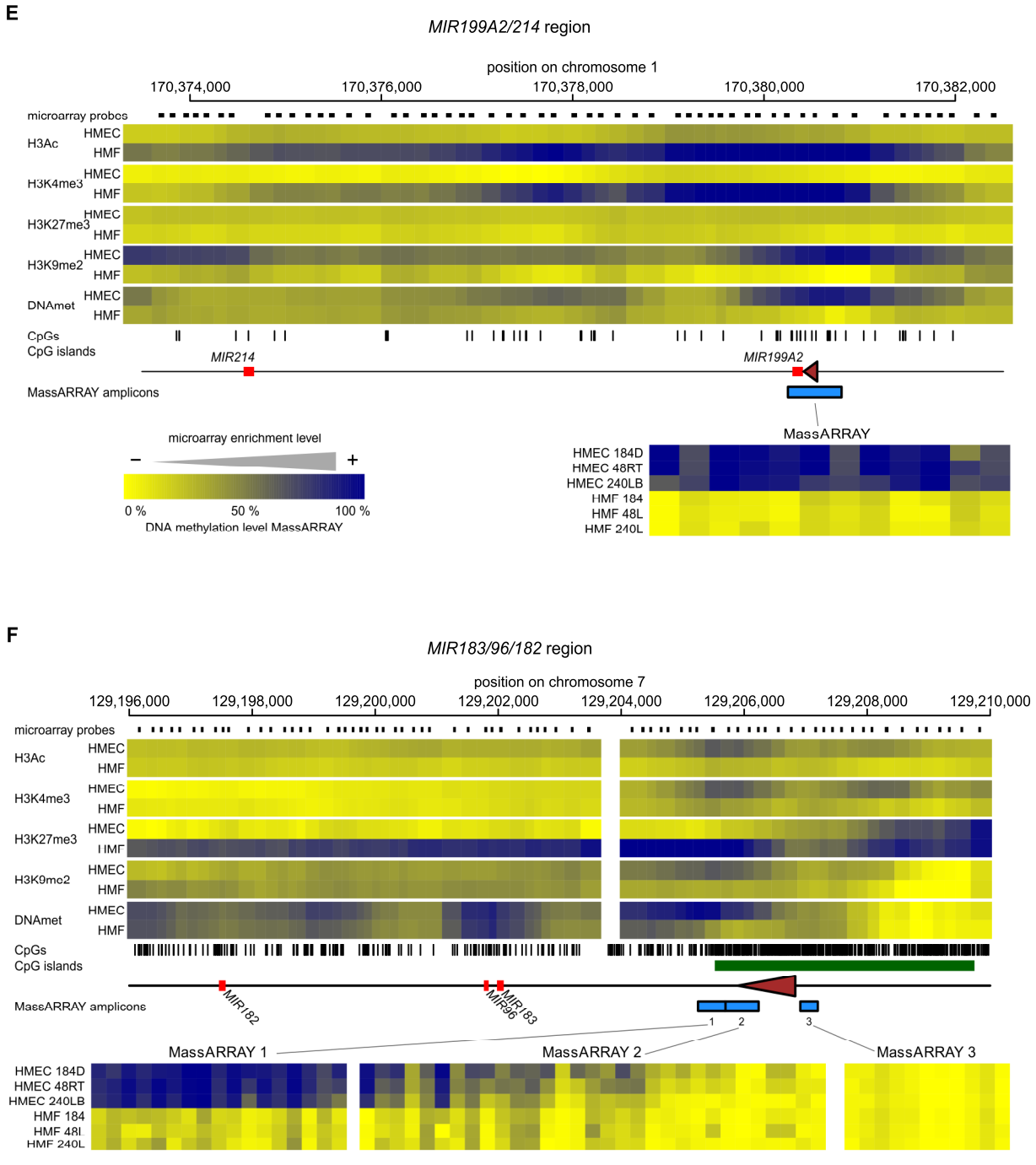
E
MIR199A2/214 region
position on chromosome 1
170,374,000
170,376,000
170,378,000
170,380,000
170,382,000
microarray probes
H3Ac
H3K4me3
H3K27me3
H3K9me2
DNAmet
HMEC
HMF
CpGs
CpG islands
MIR214
MIR199A2
MassARRAY amplicons
MassARRAY
microarray enrichment level
0 %
50 %
100 %
DNA methylation level MassARRAY
HMEC 184D
HMEC 48RT
HMEC 240LB
HMF 184
HMF 48L
HMF 240L
F
MIR183/96/182 region
position on chromosome 7
129,196,000
129,198,000
129,200,000
129,202,000
129,204,000
129,206,000
129,208,000
129,210,000
MIR182
MIR96
MIR183
MassARRAY 1
MassARRAY 2
MassARRAY 3

REFERENCES

Baffa R, Fassan M, Volinia S, O'Hara B, Liu CG, Palazzo JP, Gardiman M, Rugge M, Gomella LG, Croce CM et al. 2009. MicroRNA expression profiling of human metastatic cancers identifies cancer gene targets. *J Pathol* **219**(2): 214-221.

Bird A. 2002. DNA methylation patterns and epigenetic memory. *Genes Dev* **16**(1): 6-21.

Bueno MJ, Perez de Castro I, Gomez de Cedron M, Santos J, Calin GA, Cigudosa JC, Croce CM, Fernandez-Piqueras J, Malumbres M. 2008. Genetic and epigenetic silencing of microRNA-203 enhances ABL1 and BCR-ABL1 oncogene expression. *Cancer Cell* **13**(6): 496-506.

Epsztejn-Litman S, Feldman N, Abu-Remaileh M, Shufaro Y, Gerson A, Ueda J, Deplus R, Fuks F, Shinkai Y, Cedar H et al. 2008. De novo DNA methylation promoted by G9a prevents reprogramming of embryonically silenced genes. *Nat Struct Mol Biol* **15**(11): 1176-1183.

Friedman RC, Farh KK, Burge CB, Bartel DP. 2009. Most mammalian mRNAs are conserved targets of microRNAs. *Genome Res* **19**(1): 92-105.

Garbe JC, Bhattacharya S, Merchant B, Bassett E, Swisshelm K, Feiler HS, Wyrobek AJ, Stampfer MR. 2009. Molecular distinctions between stasis and telomere attrition senescence barriers shown by long-term culture of normal human mammary epithelial cells. *Cancer Res* **69**(19): 7557-7568.

Gardiner-Garden M, Frommer M. 1987. CpG islands in vertebrate genomes. *J Mol Biol* **196**(2): 261-282.

Gee HE, Camps C, Buffa FM, Colella S, Sheldon H, Gleadle JM, Ragoussis J, Harris AL. 2008. MicroRNA-10b and breast cancer metastasis. *Nature* **455**(7216): E8-9; author reply E9.

Greene SB, Herschkowitz JI, Rosen JM. 2010. The ups and downs of miR-205: identifying the roles of miR-205 in mammary gland development and breast cancer. *RNA Biol* **7**(3): 300-304.

Gregory PA, Bert AG, Paterson EL, Barry SC, Tsykin A, Farshid G, Vadas MA, Khew-Goodall Y, Goodall GJ. 2008a. The miR-200 family and miR-205 regulate epithelial to mesenchymal transition by targeting ZEB1 and SIP1. *Nat Cell Biol* **10**(5): 593-601.

Gregory PA, Bracken CP, Bert AG, Goodall GJ. 2008b. MicroRNAs as regulators of epithelial-mesenchymal transition. *Cell Cycle* **7**(20): 3112-3118.

Guenther MG, Levine SS, Boyer LA, Jaenisch R, Young RA. 2007. A chromatin landmark and transcription initiation at most promoters in human cells. *Cell* **130**(1): 77-88.

Hawkins RD, Hon GC, Lee LK, Ngo Q, Lister R, Pelizzola M, Edsall LE, Kuan S, Luu Y, Klugman S et al. 2010. Distinct epigenomic landscapes of pluripotent and lineage-committed human cells. *Cell Stem Cell* **6**(5): 479-491.

Heintzman ND, Stuart RK, Hon G, Fu Y, Ching CW, Hawkins RD, Barrera LO, Van Calcar S, Qu C, Ching KA et al. 2007. Distinct and predictive chromatin signatures of transcriptional promoters and enhancers in the human genome. *Nat Genet* **39**(3): 311-318.

Iorio MV, Casalini P, Piovan C, Di Leva G, Merlo A, Triulzi T, Menard S, Croce CM, Tagliabue E. 2009. microRNA-205 regulates HER3 in human breast cancer. *Cancer Res* **69**(6): 2195-2200.

Iorio MV, Piovan C, Croce CM. 2010. Interplay between microRNAs and the epigenetic machinery: an intricate network. *Biochim Biophys Acta* **1799**(10-12): 694-701.

Jaenisch R, Bird A. 2003. Epigenetic regulation of gene expression: how the genome integrates intrinsic and environmental signals. *Nat Genet* **33 Suppl**: 245-254.

Kozaki K, Imoto I, Mogi S, Omura K, Inazawa J. 2008. Exploration of tumor-suppressive microRNAs silenced by DNA hypermethylation in oral cancer. *Cancer Res* **68**(7): 2094-2105.

Laurent L, Wong E, Li G, Huynh T, Tsirigos A, Ong CT, Low HM, Kin Sung KW, Rigoutsos I, Loring J et al. 2010. Dynamic changes in the human methylome during differentiation. *Genome Res* **20**(3): 320-331.

Liang G, Lin JC, Wei V, Yoo C, Cheng JC, Nguyen CT, Weisenberger DJ, Egger G, Takai D, Gonzales FA et al. 2004. Distinct localization of histone H3 acetylation and H3-K4 methylation to the transcription start sites in the human genome. *Proc Natl Acad Sci U S A* **101**(19): 7357-7362.

Lister R, Pelizzola M, Dowen RH, Hawkins RD, Hon G, Tonti-Filippini J, Nery JR, Lee L, Ye Z, Ngo QM et al. 2009. Human DNA methylomes at base resolution show widespread epigenomic differences. *Nature* **462**(7271): 315-322.

Lujambio A, Calin GA, Villanueva A, Ropero S, Sanchez-Cespedes M, Blanco D, Montuenga LM, Rossi S, Nicoloso MS, Faller WJ et al. 2008. A microRNA DNA methylation signature for human cancer metastasis. *Proc Natl Acad Sci U S A* **105**(36): 13556-13561.

Lund AH. 2010. miR-10 in development and cancer. *Cell Death Differ* **17**(2): 209-214.

Ma L, Teruya-Feldstein J, Weinberg RA. 2007. Tumour invasion and metastasis initiated by microRNA-10b in breast cancer. *Nature* **449**(7163): 682-688.

Ma L, Weinberg RA. 2008. MicroRNAs in malignant progression. *Cell Cycle* **7**(5): 570-572.

Marson A, Levine SS, Cole MF, Frampton GM, Brambrink T, Johnstone S, Guenther MG, Johnston WK, Wernig M, Newman J et al. 2008. Connecting microRNA genes to the core transcriptional regulatory circuitry of embryonic stem cells. *Cell* **134**(3): 521-533.

Miranda TB, Jones PA. 2007. DNA methylation: the nuts and bolts of repression. *J Cell Physiol* **213**(2): 384-390.

Novak P, Jensen TJ, Garbe JC, Stampfer MR, Futscher BW. 2009. Stepwise DNA methylation changes are linked to escape from defined proliferation barriers and mammary epithelial cell immortalization. *Cancer Res* **69**(12): 5251-5258.

Oshiro MM, Watts GS, Wozniak RJ, Junk DJ, Munoz-Rodriguez JL, Domann FE, Futscher BW. 2003. Mutant p53 and aberrant cytosine methylation cooperate to silence gene expression. *Oncogene* **22**(23): 3624-3634.

Ozsolak F, Poling LL, Wang Z, Liu H, Liu XS, Roeder RG, Zhang X, Song JS, Fisher DE. 2008. Chromatin structure analyses identify miRNA promoters. *Genes Dev* **22**(22): 3172-3183.

Park SM, Gaur AB, Lengyel E, Peter ME. 2008. The miR-200 family determines the epithelial phenotype of cancer cells by targeting the E-cadherin repressors ZEB1 and ZEB2. *Genes Dev* **22**(7): 894-907.

Peter ME. 2009. Let-7 and miR-200 microRNAs: guardians against pluripotency and cancer progression. *Cell Cycle* **8**(6): 843-852.

R_Development_Core_Team. 2011. R: A Language and Environment for Statistical Computing. R Foundation for Statistical Computing, Vienna, Austria.

Rauch T, Wang Z, Zhang X, Zhong X, Wu X, Lau SK, Kernstine KH, Riggs AD, Pfeifer GP. 2007. Homeobox gene methylation in lung cancer studied by genome-wide analysis with a microarray-based methylated CpG island recovery assay. *Proc Natl Acad Sci U S A* **104**(13): 5527-5532.

Simon JA, Kingston RE. 2009. Mechanisms of polycomb gene silencing: knowns and unknowns. *Nat Rev Mol Cell Biol* **10**(10): 697-708.

Tachibana M, Sugimoto K, Nozaki M, Ueda J, Ohta T, Ohki M, Fukuda M, Takeda N, Niida H, Kato H et al. 2002. G9a histone methyltransferase plays a dominant role in euchromatic histone H3 lysine 9 methylation and is essential for early embryogenesis. *Genes Dev* **16**(14): 1779-1791.

Tellez CS, Juri DE, Do K, Bernauer AM, Thomas CL, Damiani LA, Tessema M, Leng S, Belinsky SA. 2011. EMT and stem cell-like properties associated with miR-205 and miR-200 epigenetic silencing are early manifestations during carcinogen-induced transformation of human lung epithelial cells. *Cancer Res* **71**(8): 3087-3097.

Tian Y, Luo A, Cai Y, Su Q, Ding F, Chen H, Liu Z. 2010. MicroRNA-10b promotes migration and invasion through KLF4 in human esophageal cancer cell lines. *J Biol Chem* **285**(11): 7986-7994.

Vrba L, Jensen TJ, Garbe JC, Heimark RL, Cress AE, Dickinson S, Stampfer MR, Futscher BW. 2010. Role for DNA methylation in the regulation of miR-200c and miR-141 expression in normal and cancer cells. *PLoS One* **5**(1): e8697.

Vrba L, Junk DJ, Novak P, Futscher BW. 2008. p53 induces distinct epigenetic states at its direct target promoters. *BMC Genomics* **9**: 486.

Weber M, Davies JJ, Wittig D, Oakeley EJ, Haase M, Lam WL, Schubeler D. 2005. Chromosome-wide and promoter-specific analyses identify sites of differential DNA methylation in normal and transformed human cells. *Nat Genet* **37**(8): 853-862.

Wu H, Coskun V, Tao J, Xie W, Ge W, Yoshikawa K, Li E, Zhang Y, Sun YE. 2010. Dnmt3a-dependent nonpromoter DNA methylation facilitates transcription of neurogenic genes. *Science* **329**(5990): 444-448.

Supplemental methods

Real-time PCR detection of miRNA expression

Total RNA from HMEC or HMF was extracted using the miRNeasy kit (Qiagen, Valencia, CA, USA)) according to manufacturer protocol except that Trizol (Invitrogen, Carlsbad, CA, USA) was used instead of Qiazol for the cell lysis.

Detection of microRNAs was performed using EXIQON miRCURY LNA™ Universal RT kit and individual microRNA LNA™ primer sets. Real-time PCR was conducted on an ABI Prism 7500 Sequence Detection System (Applied Biosystems, Foster City, CA, USA) using PerfeCta SYBR Green SuperMix, Low ROX (Quanta Biosciences, Gaithersburg, MD, USA) with a 95°C denaturation for 3 minutes followed by 40 cycles of 95°C for 15 seconds and 60°C for 45 seconds. Differences in expression were determined using the comparative Ct method described in the ABI user manual. SNORD44 expression was used for normalization of RNA load.

Supplemental Figure 1

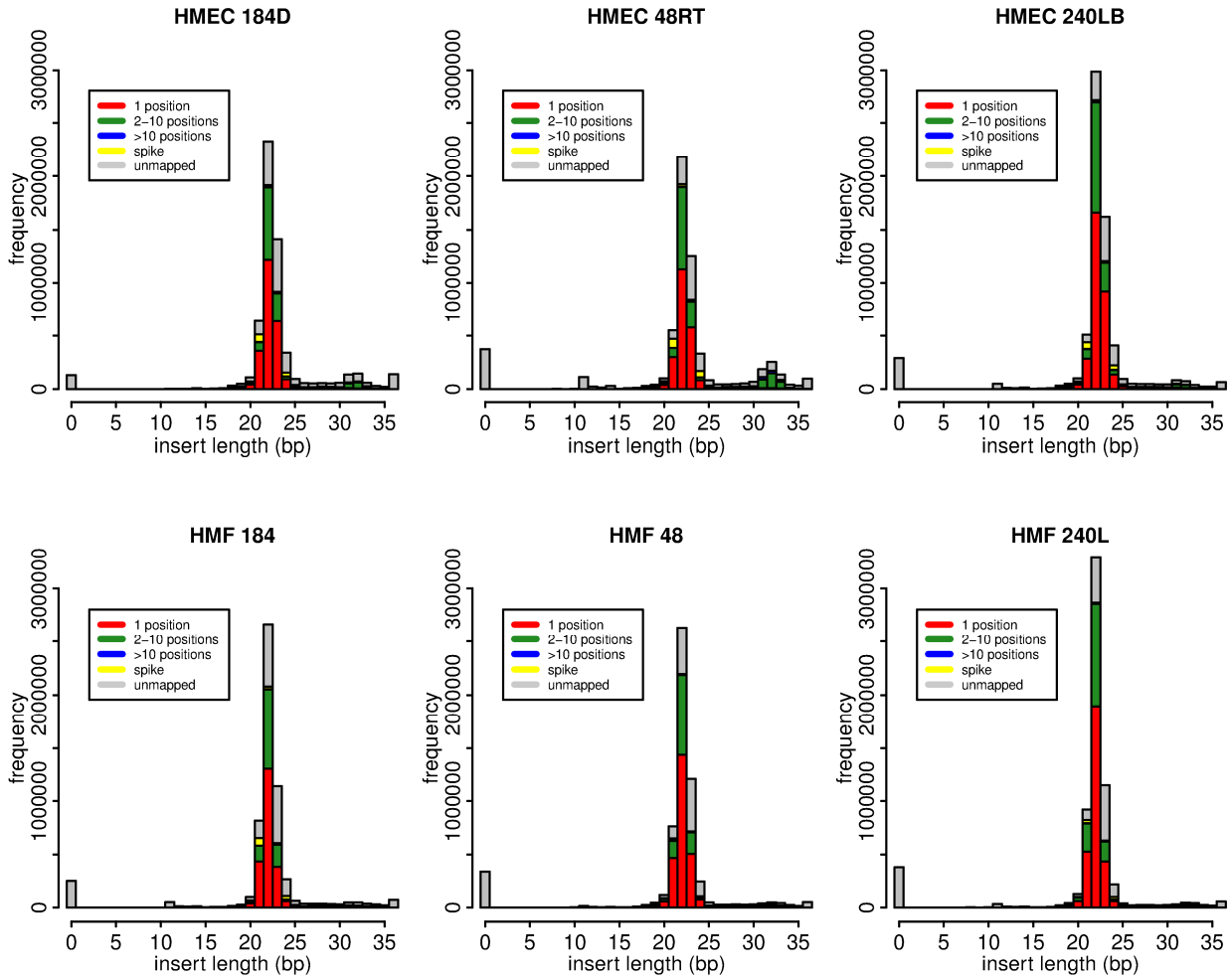

The length distribution of reads in individual libraries and proportion of the reads that were aligned to the reference genome assembly hg18. Each of six libraries provided about 6 million reads on single lane of Illumina Genome Analyzer. About 4 million (65%) of reads had perfect alignment to human genome for each sample after stripping out adaptor sequences. Most aligned reads were in the length range from 20 to 24 bp with predominant length 22 bp characteristic of miRNAs. Colors depict how the individual reads were aligned to the genome. Unmapped reads (grey) did not pass the stringent criteria for alignment. Spike (yellow) is the sequence which was added to RNA as a size marker before library construction. 65% of aligned reads (about 2.6 million/sample) have single unique location in human genome (red color). 99% of aligned reads had 10 or less perfect matches in the genome i.e. were not derived from highly repetitive sequences, but rather from single genes and gene families like miRNAs. These reads with up to ten alignments in human genome were used for further data analysis (red and green color in histograms).

Supplemental Table 1

	HMF 184	HMEC 184D	HMF 48	HMEC 48RT	HMF 240L	HMEC 240LB
Total reads	5,863,070	5,987,764	5,836,364	6,178,776	6,604,437	6,762,277
Aligned reads	3,516,718	3,758,705	3,882,756	3,840,578	4,628,163	4,794,788
Unique alignment	2,290,501	2,457,012	2,617,724	2,244,405	3,049,387	3,187,539
Filtered reads	3,492,573	3,713,580	3,854,941	3,745,091	4,601,153	4,753,694
miRNA reads	3,328,392	3,367,943	3,657,826	3,251,305	4,403,186	4,455,103

The number of reads in individual small RNA libraries. Total reads specifies the number of reads obtained, aligned reads is the number of reads with perfect match to human genome (hg18). 65% of aligned reads (about 2.6 million/sample) have single unique location in human genome (Unique alignment). 99% of aligned reads had 10 or less perfect matches in the genome i.e. were not derived from highly repetitive sequences, but rather from single genes and gene families like miRNAs. These reads were used for further analysis (Filtered reads - library size). miRNA reads is the number of reads that were mapped to known miRNA coding regions.

Supplemental Figure 2

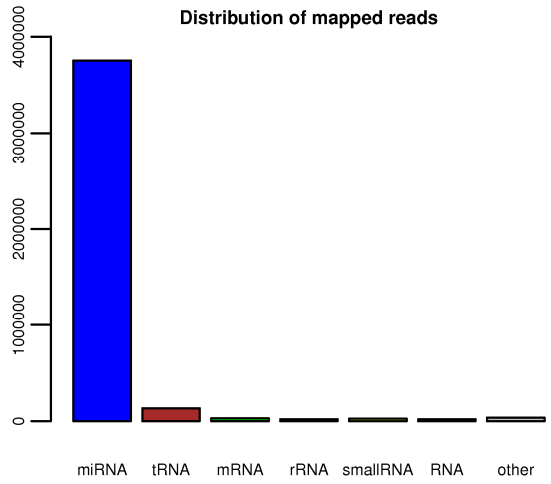

The distribution of aligned reads into individual RNA types for average library indicating high proportion of miRNAs. Over 90% of the aligned reads (over 3.7 million/sample) mapped to annotated miRNA regions. Majority of the reads that did not align to miRNA regions were fragments of tRNA (3.3% of library), mRNA (0.7% of library), rRNA (0.5% of library), other small RNA or other RNA with about 0.9% reads in non annotated regions.

Supplemental Figure 3

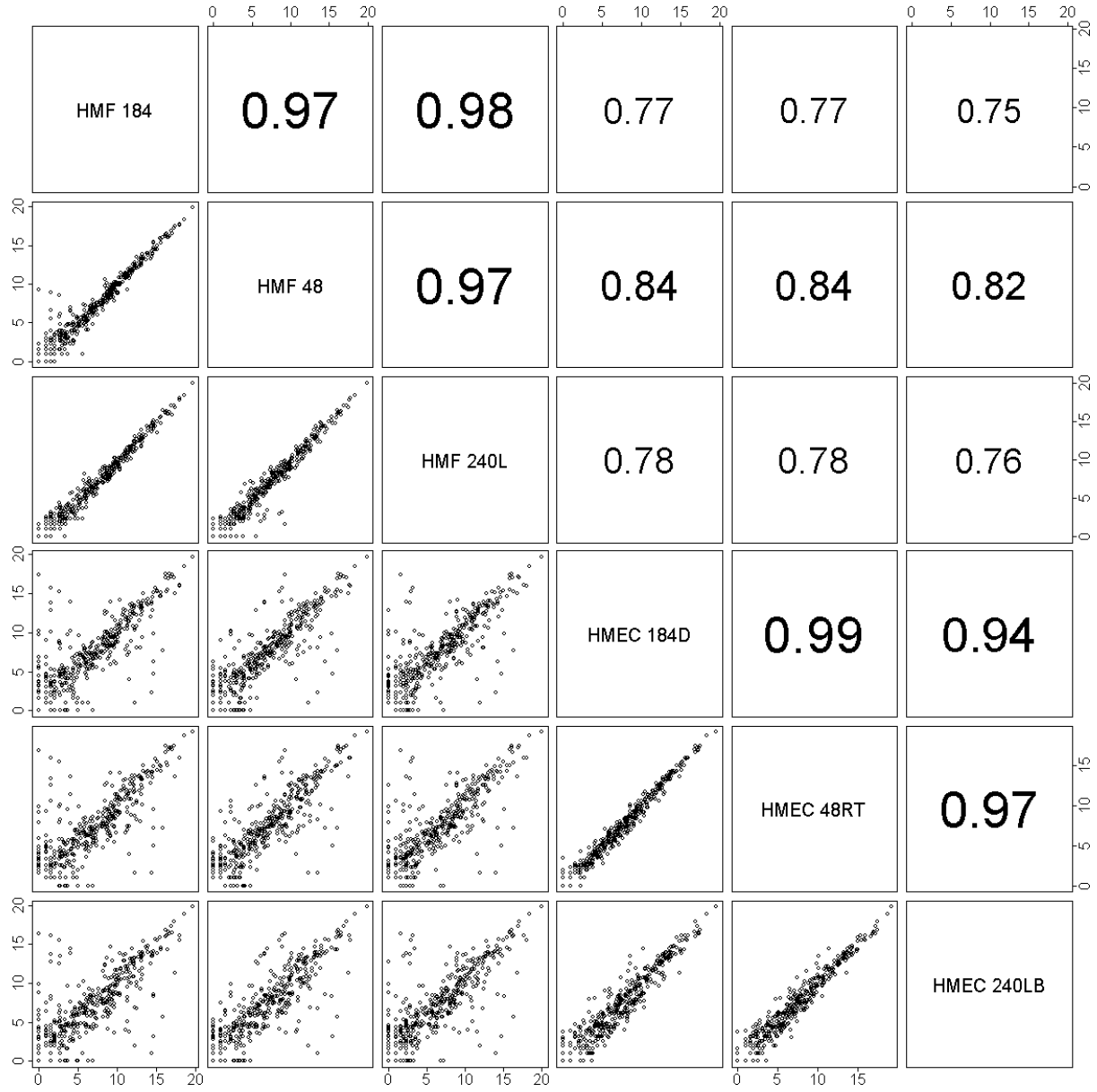

The correlation between miRNA expression in individual samples.

Supplemental Figure 4

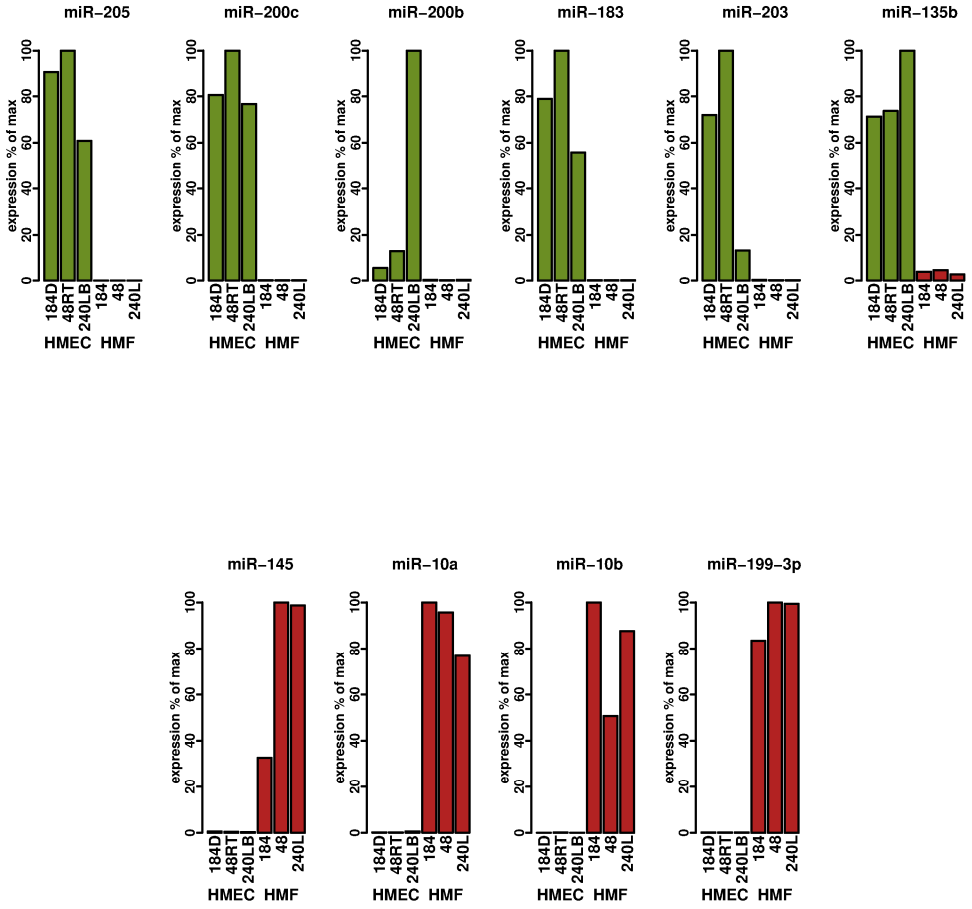

Real-time PCR verification of the expression of selected tissue specific miRNAs. Data are normalized to the highest expressing sample for each miRNA (100 %). The individual HMEC samples are in green, their paired HMF samples are in red. The data are in high concordance with the data obtained by miRNA library sequencing.

Supplemental Figure 5

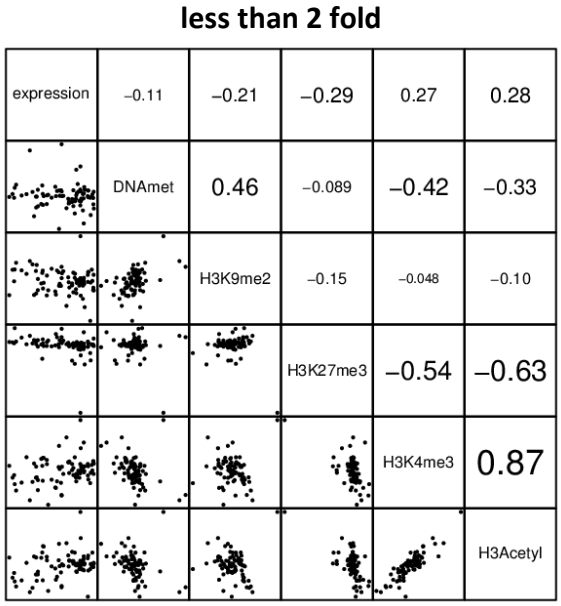

Differences in HMEC/HMF miRNA expression correlated with differences in epigenetic marks at their promoters for miRNA genes that were not differentially expressed. We used data from all probes within a 2 kb region centered on the predicted TSS region and calculated the correlation of difference in enrichment of individual epigenetic marks between the cell types. Only miRNA genes with 2 fold or lower difference in expression are shown. The numbers show correlation coefficients for individual pairs of epigenetic marks.

Supplemental Figure 6

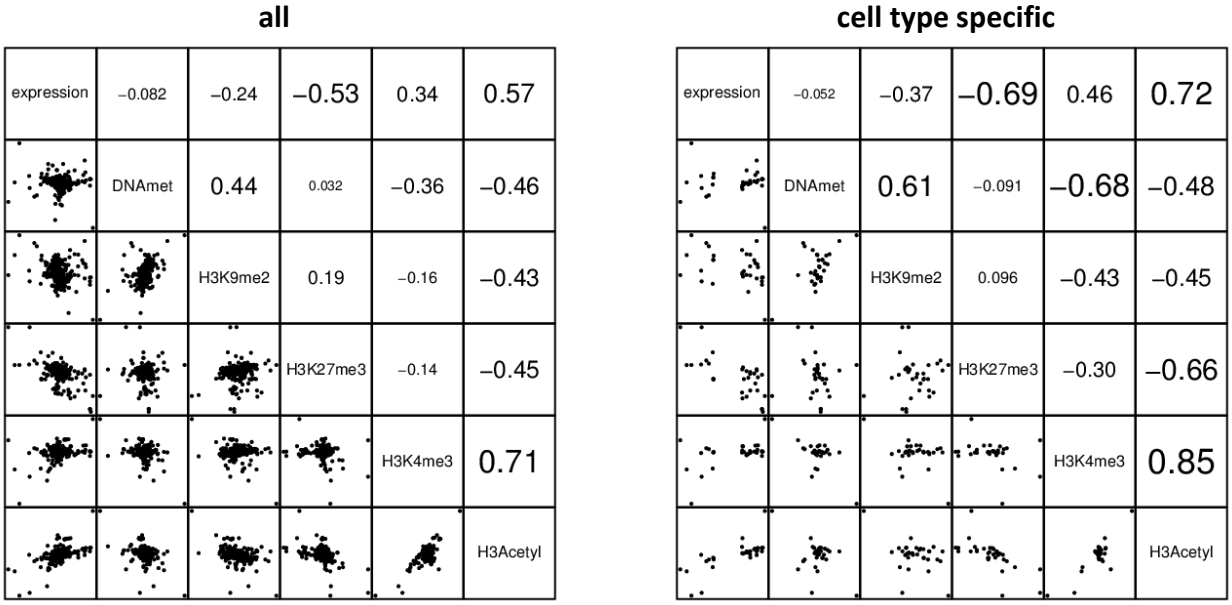

Differences in HMEC/HMF miRNA expression correlated with differences in epigenetic marks at miRNA hairpin coding regions. We used data from all probes within a 2 kb region centered on the miRNA hairpin coding regions and calculated the correlation of difference in enrichment of individual epigenetic marks between the cell types. Only hairpins located 2 or more kb from promoter region were used for analysis, so the analyzed regions do not overlap with promoter regions. The left panel shows correlations for all miRNA hairpin regions and the right panel shows cell type specific miRNA hairpin regions only.

Supplemental Figure 7

A

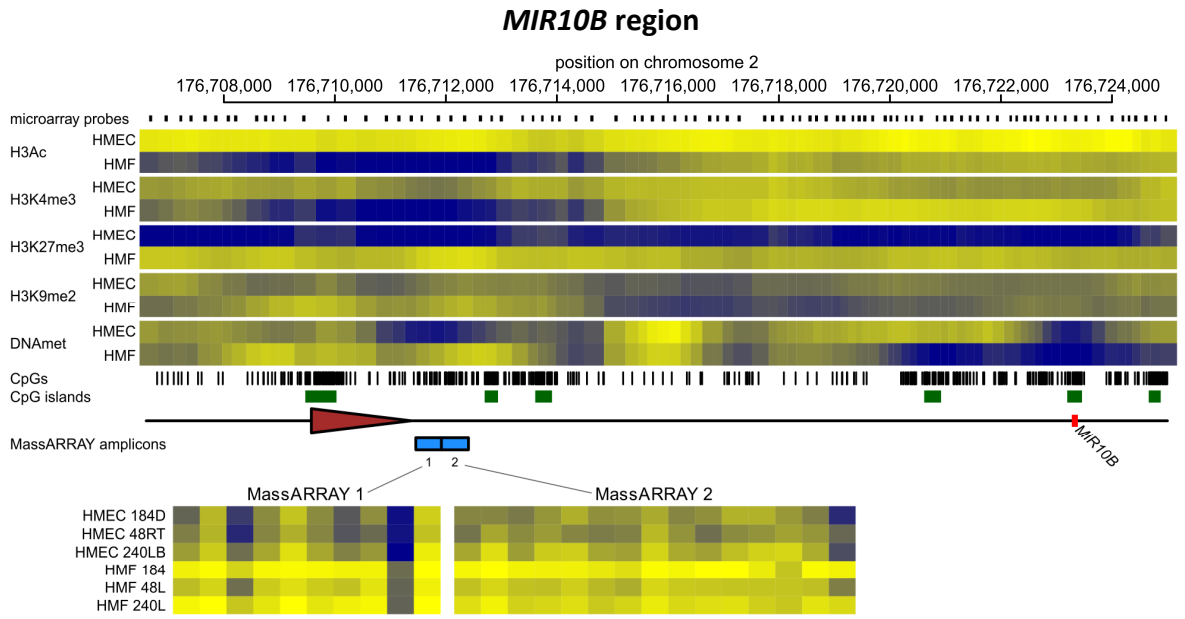

B

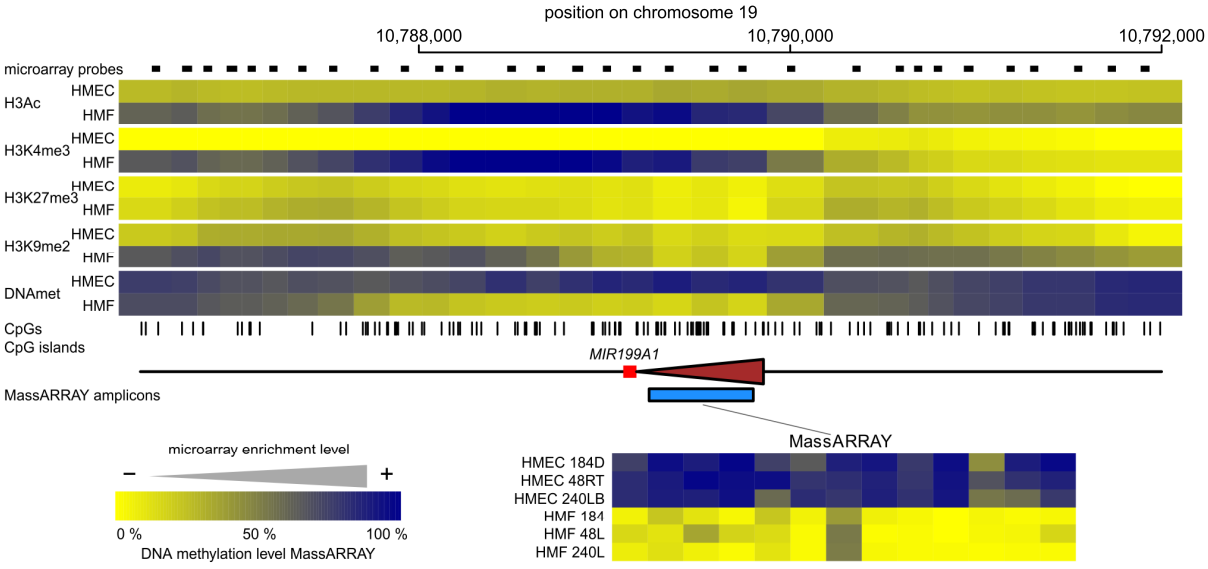

Supplemental Figure 7

C

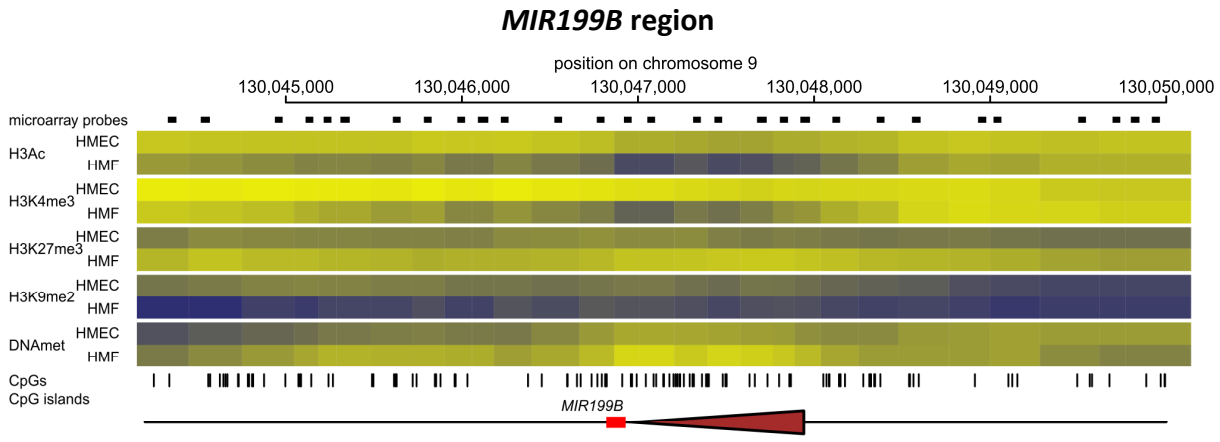

Supplemental Figure 7 The epigenetic state of cell type specific miRNA genes in HMEC and HMF. Top part shows the enrichment of individual epigenetic marks through the regions in a heatmap form, with yellow indicating no enrichment and blue color indicating high enrichment. The data for HMEC and HMF samples are averages from three genotypes of HMEC and HMF respectively. The miRNA hairpin coding regions are displayed as a red rectangles and predicted transcription start site regions as brown triangles. Small black rectangles at the top lane indicate positions of individual microarray probes. The tics at the bottom indicate positions of individual CpG dinucleotides. CpG islands according to UCSC are displayed as green rectangles when present. The blue rectangle at the bottom lane indicates position of region analyzed for DNA methylation by MassARRAY technology. Results from MassARRAY for this region is shown at the bottom part. The level of methylation of individual CpG units within the MassARRAY amplicon is displayed as a heatmap with the lowest methylation (0%) in yellow and the highest methylation (100%) in blue. The individual samples are labeled on the left side. The individual CpG units are marked at the bottom.

Supplemental Figure 8

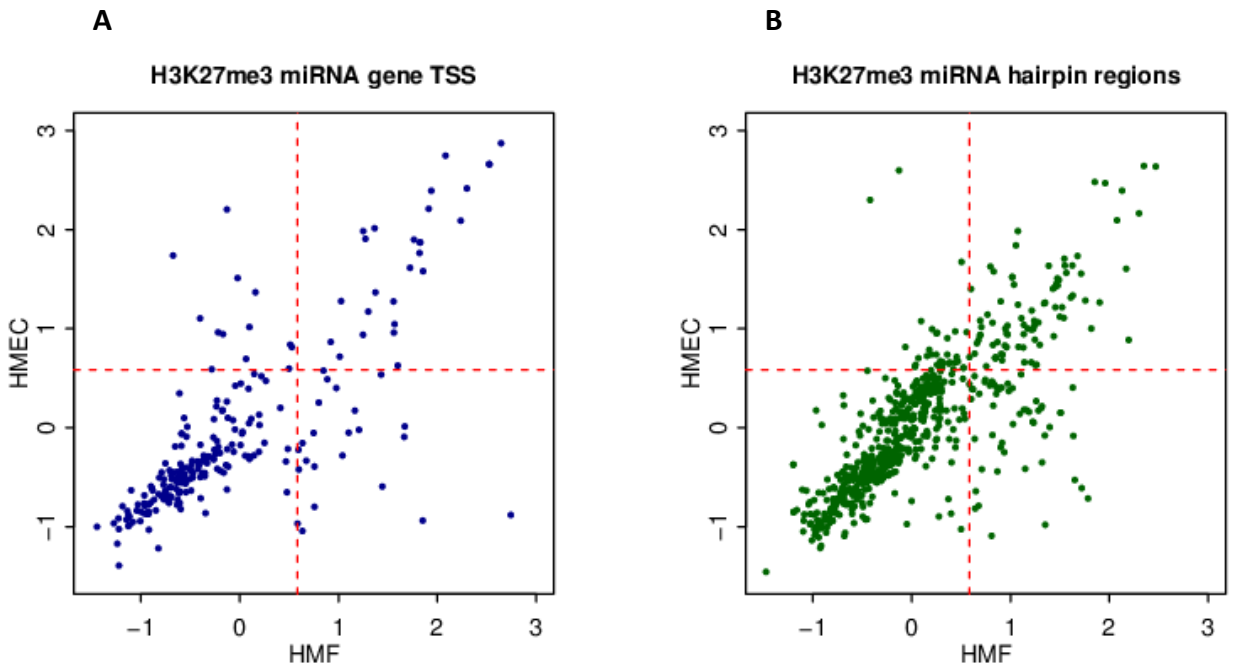

The presence of H3K27me3 on individual miRNA gene TSS regions (A) and miRNA encoding hairpin regions (B) for HMF and HMEC. The axes show enrichment of H3K27me3 over input for HMF and HMEC in logarithmic scale. The data were collected from 2 kb region centered on TSS or hairpin region of individual miRNAs. The horizontal and vertical lines indicate log2(1.5) i.e. 1.5 fold enrichment over input, which was considered a threshold. The proportion of analyzed regions occupied by H3K27me3 in either or both cell types was 27.5% and 26.9% for TSS and hairpin regions respectively.

Supplemental Table 2

List of tissue specific miRNAs found deregulated in cancer

miR-10a	- (Veerla et al. 2009; Weiss et al. 2009)
miR-10b	- (Ma et al. 2007; Baffa et al. 2009)
miR-135b	- (Guled et al. 2009; Sarver et al. 2009)
miR-143/145	- (Iorio et al. 2007; Nam et al. 2008; Baffa et al. 2009)
miR-183/96/182	- (Nakada et al. 2008; Nikiforova et al. 2008; Sarver et al. 2009; Shimono et al. 2009)
miR-195/497	- (Li et al. 2011)
miR-199 family	- (Iorio et al. 2007; Nakada et al. 2008; Nam et al. 2008; Yang et al. 2008; Yin et al. 2010)
miR-200 family	- (Iorio et al. 2007; Gregory et al. 2008; Nakada et al. 2008; Nam et al. 2008; Park et al. 2008; Baffa et al. 2009; Du et al. 2009; Kong et al. 2009; Shimono et al. 2009; Vrba et al. 2010; Castilla et al. 2011)
miR-203	- (Baffa et al. 2009; Guled et al. 2009; Castilla et al. 2011)
miR-205	- (Nikiforova et al. 2008; Baffa et al. 2009; Childs et al. 2009; Gandellini et al. 2009; Iorio et al. 2009)
miR-210	- (Nakada et al. 2008; Greither et al. 2011)
miR-214	- (Yang et al. 2008; Yin et al. 2010)
miR-187	- (Nakada et al. 2008; Nikiforova et al. 2008)
miR-378	- (Sarver et al. 2009)
miR-424	- (Yang et al. 2008)
miR-450a	- (Castilla et al. 2011)
miR-542-5p	- (Castilla et al. 2011)
miR-582	- (Guled et al. 2009)
miR-584	- (Ueno et al. 2011)

Supplemental Data 1

Expression for all miRNAs for all samples. The numbers in columns show the counts of individual miRNAs in individual small RNA libraries normalized for average library size. Separate file in excel format.

Supplemental Data 2

Positions of predicted miRNA promoter regions. Coordinates are valid for human genome assembly hg18. Separate file in .bed format.

Supplemental Table 3

Positions of MassARRAY amplicons in hg18 and sequences of MassARRAY primers used for DNA methylation analysis

chr	start	end	amplicon name	10F primer sequence	T7R primer sequence
chr1	1087874	1088338	mir-200b/200a/429_1	aggaagagagGGAGTTGGGTGTTTTGTTTTAGTTA	cagtaatacgactcactatagggagaaggctAAAAACCTTCCCATCCTAACTTTTA
chr1	1089747	1090248	mir-200b/200a/429_2	aggaagagagGATTTTTGGAGGAGTTGGTGTG	cagtaatacgactcactatagggagaaggctAAAATAAATCAAAAAACCCAAAACC
chr1	1091032	1091557	mir-200b/200a/429_3	aggaagagagGTTTTTGAAGTATTGATTTGATGGG	cagtaatacgactcactatagggagaaggctCTACCTAAAACCCAAAAACCCTAAA
chr1	1091920	1092393	mir-200b/200a/429_4	aggaagagagGGGTAGGGAAGTAGTTTTTGGAATA	cagtaatacgactcactatagggagaaggctCTCCATCCAATACTACCCAATAAAA
chr1	170380250	170380811	mir-199a-2/214	aggaagagagTGGGGTTTATTTTTTGTTTAGTTGA	cagtaatacgactcactatagggagaaggctATCTTCTCCTTAAAAACAACCCATT
chr1	207667743	207668344	mir-205_1	aggaagagagTAGTTTTATGAAGGGTTGTGGGATA	cagtaatacgactcactatagggagaaggctAAATCCAACAAAAATAAACCAATCC
chr1	207668250	207668816	mir-205_2	aggaagagagATGTTAGGATAAGTTTTTGGTTGGG	cagtaatacgactcactatagggagaaggctTAAACAAAAAAAACTCAACCCATTT
chr1	207672053	207672526	mir-205_3	aggaagagagTGTAGTGTTTATAGGTTGAGGTTGA	cagtaatacgactcactatagggagaaggctCAAAAAAACTTTTCAATAAACAAACAAC
chr2	176711458	176711922	mir-10b_1	aggaagagagTGGATAGTGGTTTTTAGGTTTTGTT	cagtaatacgactcactatagggagaaggctTAAACTTCTCAACTCTCAAAATCCC
chr2	176711919	176712407	mir-10b_2	aggaagagagAAAGGATTAGTTTTTAGAAAGAGGG	cagtaatacgactcactatagggagaaggctCCCAAAAATATAACTCCCAATATCC
chr7	129205249	129205696	mir-183/96/182_1	aggaagagagATGTTTTTGAGGTTTTAGGGGTTAG	cagtaatacgactcactatagggagaaggctAAACCTACCCCAAACCCAACTCT
chr7	129205680	129206235	mir-183/96/182_2	aggaagagagGGGTTTGGGGTAGGTTTTTTT	cagtaatacgactcactatagggagaaggctCTAATAACACCCAAATTCCCAAC
chr7	129206913	129207197	mir-183/96/182_3	aggaagagagGGAGTTTATATTAGAGAAGTTAGGTAAAAA	cagtaatacgactcactatagggagaaggctAACCCAAATACCCCTCTAAACCT
chr12	6942734	6943252	mir-200c	aggaagagagGTTGTAGTTAGTTAAGGGTTGGGGA	cagtaatacgactcactatagggagaaggctCAACACCCACTCTCTAAAAACAAAT
chr17	44014859	44015307	mir-10a	aggaagagagTTTTGGTAGTTTTTGTTAAATAGTTAGG	cagtaatacgactcactatagggagaaggctTACCCAAAACCATACTTTCAATTTT
chr19	10789240	10789801	mir-199a-1	aggaagagagTAAGGTTGGGTAATATAGGGTTTGG	cagtaatacgactcactatagggagaaggctCAACACCTCTAAACAACCAAAAAAA

Supplemental References

Baffa R, Fassan M, Volinia S, O'Hara B, Liu CG, Palazzo JP, Gardiman M, Rugge M, Gomella LG, Croce CM et al. 2009. MicroRNA expression profiling of human metastatic cancers identifies cancer gene targets. *J Pathol* **219**(2): 214-221.

Castilla MA, Moreno-Bueno G, Romero-Perez L, Van De Vijver K, Biscuola M, Lopez-Garcia MA, Prat J, Matias-Guiu X, Cano A, Oliva E et al. 2011. Micro-RNA signature of the epithelial-mesenchymal transition in endometrial carcinosarcoma. *J Pathol* **223**(1): 72-80.

Childs G, Fazzari M, Kung G, Kawachi N, Brandwein-Gensler M, McLemore M, Chen Q, Burk RD, Smith RV, Prystowsky MB et al. 2009. Low-level expression of microRNAs let-7d and miR-205 are prognostic markers of head and neck squamous cell carcinoma. *Am J Pathol* **174**(3): 736-745.

Du Y, Xu Y, Ding L, Yao H, Yu H, Zhou T, Si J. 2009. Down-regulation of miR-141 in gastric cancer and its involvement in cell growth. *J Gastroenterol* **44**(6): 556-561.

Gandellini P, Folini M, Longoni N, Pennati M, Binda M, Colecchia M, Salvioni R, Supino R, Moretti R, Limonta P et al. 2009. miR-205 Exerts tumor-suppressive functions in human prostate through down-regulation of protein kinase Cepsilon. *Cancer Res* **69**(6): 2287-2295.

Gregory PA, Bert AG, Paterson EL, Barry SC, Tsykin A, Farshid G, Vadas MA, Khew-Goodall Y, Goodall GJ. 2008. The miR-200 family and miR-205 regulate epithelial to mesenchymal transition by targeting ZEB1 and SIP1. *Nat Cell Biol* **10**(5): 593-601.

Greither T, Wurl P, Grochola L, Bond G, Bache M, Kappler M, Lautenschlager C, Holzhausen HJ, Wach S, Eckert AW et al. 2011. Expression of microRNA 210 associates with poor survival and age of tumor onset of soft-tissue sarcoma patients. *Int J Cancer*.

Guled M, Lahti L, Lindholm PM, Salmenkivi K, Bagwan I, Nicholson AG, Knuutila S. 2009. CDKN2A, NF2, and JUN are dysregulated among other genes by miRNAs in malignant mesothelioma -A miRNA microarray analysis. *Genes Chromosomes Cancer* **48**(7): 615-623.

Iorio MV, Casalini P, Piovan C, Di Leva G, Merlo A, Triulzi T, Menard S, Croce CM, Tagliabue E. 2009. microRNA-205 regulates HER3 in human breast cancer. *Cancer Res* **69**(6): 2195-2200.

Iorio MV, Visone R, Di Leva G, Donati V, Petrocca F, Casalini P, Taccioli C, Volinia S, Liu CG, Alder H et al. 2007. MicroRNA signatures in human ovarian cancer. *Cancer Res* **67**(18): 8699-8707.

Kong D, Li Y, Wang Z, Banerjee S, Ahmad A, Kim HR, Sarkar FH. 2009. miR-200 Regulates PDGF-D-Mediated Epithelial-Mesenchymal Transition, Adhesion, and Invasion of Prostate Cancer Cells. *Stem Cells* **27**(8): 1712-1721.

Li D, Zhao Y, Liu C, Chen X, Qi Y, Jiang Y, Zou C, Zhang X, Liu S, Wang X et al. 2011. Analysis of MiR-195 and MiR-497 expression, regulation and role in breast cancer. *Clin Cancer Res* **17**(7): 1722-1730.

Ma L, Teruya-Feldstein J, Weinberg RA. 2007. Tumour invasion and metastasis initiated by microRNA-10b in breast cancer. *Nature* **449**(7163): 682-688.

Nakada C, Matsuura K, Tsukamoto Y, Tanigawa M, Yoshimoto T, Narimatsu T, Nguyen LT, Hijiya N, Uchida T, Sato F et al. 2008. Genome-wide microRNA expression profiling in renal cell carcinoma: significant down-regulation of miR-141 and miR-200c. *J Pathol* **216**(4): 418-427.

Nam EJ, Yoon H, Kim SW, Kim H, Kim YT, Kim JH, Kim JW, Kim S. 2008. MicroRNA expression profiles in serous ovarian carcinoma. *Clin Cancer Res* **14**(9): 2690-2695.

Nikiforova MN, Tseng GC, Steward D, Diorio D, Nikiforov YE. 2008. MicroRNA expression profiling of thyroid tumors: biological significance and diagnostic utility. *J Clin Endocrinol Metab* **93**(5): 1600-1608.

Park SM, Gaur AB, Lengyel E, Peter ME. 2008. The miR-200 family determines the epithelial phenotype of cancer cells by targeting the E-cadherin repressors ZEB1 and ZEB2. *Genes Dev* **22**(7): 894-907.

Sarver AL, French AJ, Borralho PM, Thayanithy V, Oberg AL, Silverstein KA, Morlan BW, Riska SM, Boardman LA, Cunningham JM et al. 2009. Human colon cancer profiles show differential microRNA expression depending on mismatch repair status and are characteristic of undifferentiated proliferative states. *BMC Cancer* **9**: 401.

Shimono Y, Zabala M, Cho RW, Lobo N, Dalerba P, Qian D, Diehn M, Liu H, Panula SP, Chiao E et al. 2009. Downregulation of miRNA-200c links breast cancer stem cells with normal stem cells. *Cell* **138**(3): 592-603.

Ueno K, Hirata H, Shahryari V, Chen Y, Zaman MS, Singh K, Tabatabai ZL, Hinoda Y, Dahiya R. 2011. Tumour suppressor microRNA-584 directly targets oncogene Rock-1 and decreases invasion ability in human clear cell renal cell carcinoma. *Br J Cancer* **104**(2): 308-315.

Veerla S, Lindgren D, Kvist A, Frigyesi A, Staaf J, Persson H, Liedberg F, Chebil G, Gudjonsson S, Borg A et al. 2009. MiRNA expression in urothelial carcinomas: important roles of miR-10a, miR-222, miR-125b, miR-7 and miR-452 for tumor stage and metastasis, and frequent homozygous losses of miR-31. *Int J Cancer* **124**(9): 2236-2242.

Vrba L, Jensen TJ, Garbe JC, Heimark RL, Cress AE, Dickinson S, Stampfer MR, Futscher BW. 2010. Role for DNA methylation in the regulation of miR-200c and miR-141 expression in normal and cancer cells. *PLoS One* **5**(1): e8697.

Weiss FU, Marques IJ, Woltering JM, Vlecken DH, Aghdassi A, Partecke LI, Heidecke CD, Lerch MM, Bagowski CP. 2009. Retinoic acid receptor antagonists inhibit miR-10a expression and block metastatic behavior of pancreatic cancer. *Gastroenterology* **137**(6): 2136-2145 e2131-2137.

Yang H, Kong W, He L, Zhao JJ, O'Donnell JD, Wang J, Wenham RM, Coppola D, Kruk PA, Nicosia SV et al. 2008. MicroRNA expression profiling in human ovarian cancer: miR-214 induces cell survival and cisplatin resistance by targeting PTEN. *Cancer Res* **68**(2): 425-433.

Yin G, Chen R, Alvero AB, Fu HH, Holmberg J, Glackin C, Rutherford T, Mor G. 2010. TWISTing stemness, inflammation and proliferation of epithelial ovarian cancer cells through MIR199A2/214. *Oncogene* **29**(24): 3545-3553.